Title
DDX3X and C12ORF57/Camkinin: Insight into the function and malfunction of two genes implicated in agenesis of the corpus callosum

Author
Jiang, Ruiji

Publication Date
2019

Peer reviewed|Thesis/dissertation

DDX3X and C12ORF57/Camkinin: Insight into the function and malfunction of two genes implicated in agenesis of the corpus callosum

by
Ruiji Jiang

DISSERTATION
Submitted in partial satisfaction of the requirements for degree of
DOCTOR OF PHILOSOPHY

in

Biomedical Sciences

in the

GRADUATE DIVISION
of the
UNIVERSITY OF CALIFORNIA, SAN FRANCISCO

Approved:

DocuSigned by:
Aimee Kao
745CF57D40DB494...
Aimee Kao
Chair

DocuSigned by:
Elliott Sherr
Elliott Sherr

DocuSigned by:
John Rubenstein

DocuSigned by:
Kevin Shannon
6F9DD324E1BF466...
Kevin Shannon

Committee Members

Acknowledgements

I would like to thank Malek Chouchane and Erik Ullian for their assistance in planning and collecting the electrophysiology data for the sections dealing with C12ORF57. The Linda Richards lab at the Queensland Brain Insitute, specifically Ching Moey and also provided valuable support in performing dual stain *in situs* and immunohistochemistry for the cell type specific expression assays as well as sectioning for mouse brains. Thanks to Suling Wong for her artistic expertise in illustrating our C12ORF57/Camkinin model

Stephen Floor and the Doudna lab at Berkeley provided invaluable assistance in explaining the principles of the DDX3X unwinding assay, as well as providing technical assistance in purifying protein, and short RNA sequences for the radioactive assay, and provided guidance. Krister Barkovitch, Megan Radler, and the Kevan Shokat lab at UCSF also provided valuable advice and access to their Tecan plate reader. The Debbie Silver lab and Ashley Lennox at Duke University provided data and expertise on DDX3X's role on neuronal migration and input in the writing of our paper and the framing of DDX3X in overall brain development.

Special thanks to the DDX3X Family foundation for providing funding towards our DDX3X research, inviting us to speak at their annual conference, and helping to coordinate and recruit patients into our DDX3X study.

Special thanks given to all members of the Sherr Lab, especially Brieana Fregeau, Lindsay Suit, Talia Beerson, Veronica Santiago, and Kendall Parks for recruiting and managing clinical data for both DDX3X and C12ORF57 projects, as well as for performing neurobehavioral assessments found in the DDX3X patients as well as other patients within our cohort.

Thanks to my thesis advisory committee Aimee Kao, John Rubenstein and Kevin Shannon for their advice, encouragement, and well considered criticism. My work would not be as complete or rigorous without your advice.

Thanks to the Moritz and Heyman Discovery Fellows program as well as the UCSF Genentech Fellows program for providing funding to me through my graduate school career.

Thanks also to my Thesis mentor Elliott Sherr who provided so much help, support, advice, throughout my PhD. None of this would be possible without the opportunity provided in the lab and if you hadn't given me those two otherwise stagnant side projects.

And finally thanks to family and specifically my mom and dad for always supporting me and encouraging me to go into science, and supporting me throughout it.

Contributions

The text of Chapter 2 is a reprint of the material as it appears in **Pathogenic *DDX3X* mutations impair RNA metabolism and neurogenesis during fetal cortical development** on *BioRXiv* (Lennox *et al*, 2018). The co-author listed in this publication directed and supervised the research that forms the basis for the chapter.

Experiments performed in Chapter 3 section Loss of C12ORF57 increases basal neuronal excitability in hippocampal neurons were performed by Malek Chouchane. Work in Chapter 3 are currently in preparation for publication.

Abstract: DDX3X and C12ORF57/Camkinin: Insight into the function and malfunction of two genes implicated in agenesis of the corpus callosum

Ruiji Jiang

Agenesis of the corpus callosum (ACC) is one of the of the most common defects of the central nervous system with an incidence of 1/20000-30000 live births, putting it behind only spinal cord defects in terms of prevalence. While many candidate genes have been identified in patients with ACC, only 30% of all cases of ACC with a suspected genetic cause have an identified candidate gene. Patients with ACC rarely have ACC in isolation and usually have other neurologic (epilepsy, intellectual disability, cortical malformations), and neurodevelopmental (autism spectrum disorder, mood disorders) problems as well. Genes implicated in agenesis of the corpus callosum vary wildly from genes implicated in neurogenesis(PAX6, DISC1), axonal targeting and interaction(L1CAM), neuronal specification(SATB2), and neuronal survival. Identifying and characterizing potential genes in ACC gives us insight into neurodevelopment as a whole. My thesis work focused on two genes implicated in agenesis of the corpus callosum whose role in brain development was heretofore unknown, DEAD-box Helicase 3 X-linked (DDX3X), an RNA helicase, and C12ORF57 which we have tentatively named Camkinin a gene which had no previously known function. My work has shown that a subset of missense mutations in DDX3X completely inhibit its RNA helicase activity, which correlates with striking brain anatomy changes and more severe clinical outcomes. I have also reported the first evidence that demonstrates a likely function for the novel protein Camkinin, suggesting that it regulates the kinase CamKIV and through that controls synaptic scaling in excitatory neurons. Thus, through the two arms of my research we were able to further elucidate the brain specific function of these proteins and discover potential therapeutic avenues for patients and give insight into pathways crucial to normal brain development.

Table of Contents

List of Figures

List of Tables

CHAPTER 1 Introduction

Genetics and Brain Development: A rapidly growing field

The study of human genetics as it applies to the brain and brain development is a rapidly developing field of study. As sequencing technology has improved, finding novel mutations in genes has become cheaper and faster. However, the majority of mutations found in genes have not had a biological consequence associated with them and moving forward the need now shifts to the characterization of these mutations. As clinical genome sequencing (both whole genome and whole exome sequencing) becomes more accessible to greater numbers of patients, the interpretation of numerous mutations of unknown significance will become increasingly more relevant to the physician. Characterization of specific mutations in genes associated with brain development will help provide patients and caregivers with information about expected development and prognosis useful for decisions regarding planning of care, parental expectations and treatment. In the past decades the study of human genomics given us multiple insights into genes necessary for normal brain development such as autism spectrum disorder(SHANK3, FMR, AIRD1B etc), Intellectual disability (DISC1, C12ORF57, DDX3Xetc) and juvenile epilepsy disorders,(GABRA1, EFHC1). While strides have been made in determining the function of some of these genes, the large number of genes have no known function or have unknown function in the brain. During my time in the Sherr lab I have worked on characterizing genes associated with dysgenesis of the corpus callosum.

Clinical Phenotype of Agenesis of the Corpus Callosum

The corpus callosum (CC), the largest commissural tract in the mammalian brain, is essential for interhemispheric integration of sensory, motor, and higher-order cognitive information containing approximately 190 million axons. (Figure 2). By radiologic convention it is divided into four segments, the rostrum, genu, body, and splenium (Gott and Saul, 1978). Recent diffusion

tensor imaging (DTI) scans have given us even more detailed insight into the organization of the fibers within the corpus callosum; they largely form symmetric homotypic connections between cortical regions with few heterotypic connections (Dorrian AA *et al.* 2000). Partial or complete agenesis of the corpus callosum (ACC) is one of the most common congenital brain malformations, present in at least 1-4000 live births, with recent actuarial data estimating ACC being present in 1:2,000 live births (Glass *et al.* 2008). Certain disorders, such as neurofibromatosis-1 and Temtamy syndrome (C12ORF57) which will be discussed in more detail later, can present with a thickened corpus callosum as well (Schlupper *et al.* 2017, Zahrani *et al.* 2013). While isolated ACC tends to have a much more moderate outcome with patients having IQs in the normal range (80-100) without other more serious neurologic sequelae (Sotirialdis *et al.*, 2012). ACC is more commonly associated with other disorders of brain development; patients often fall within the autistic spectrum, and can have anywhere between mild to severe intellectual disability. The connection between ACC and neurodevelopmental disorders is such that 3-5% of individuals assessed for neurodevelopmental disorders have ACC (Bodensteiner *et al.*, 1993, Jeret *et al.* 1985). We can therefore view syndromic dysgenesis of the corpus callosum as a highly visible consequence of an underlying disruption of neuronal connectivity and brain development. To understand why this would be the case we first must take time to understand the multiple biologic processes behind the normal development of the human corpus callosum, and the genetic and molecular basis of genes associated with agenesis of the corpus callosum in human patients.

Normal development of the corpus callosum

In human callosal development the initial axons can be seen crossing the midline at 13-14 weeks of gestation, with the anterior sections beginning to grow by weeks 14 and 15, and the posterior sections developing afterwards in weeks 18 and 19(Rakic and Yakovlev 1967, Hewit, 1962, Ren *et al.* 2006, Byrd *et al.* 1978). This two locus origin of the corpus callosum is

consistent with diffusion tensor imaging studies showing a variety of homotopic and heterotopic connections in partial ACC. The structure reaches a more complete form at 18-20 weeks of human gestation and later thickening up to 3+ years after birth, with activity dependent axonal pruning occurring throughout childhood and adolescence (Innocenti and Price 2005). While anatomical details of corpus callosum development in humans can and have been observed, mouse models of ACC have provided valuable insight into the molecular and cellular processes underlying corpus callosum development. The first step in normal callosal development is the formation of the midline within the developing forebrain, through which the axons of the corpus callosum will eventually pass. In mice, this process begins with the expression of *Fgf8* under control of SHH in the dorsal midline of the developing fore brain which commences the formation of the commissural plate, masa commusuralli, area septalis and is essential for hemispheric cleavage(Hayhurst *et al.* 2008, Okada *et al.*, 2008, Edwards *et al.*, 2014). By embryonic day 15.5 of gestation, this hemispheric cleavage and a dorsal-ventral patterning of morphogens through the developing midline structures of the massa commisuralis and area septalis develops which will later guide various commissural fibers with the corpus callosum passing dorsally through *Emx1* and *Nfia* expressing domains through the mass commisuralis (Moldrich *et al.* 2010) later on in development. By E15, midline fusion will have completed. While the evidence for how this process occurs is lacking, it appears that the midline zipper glia appear to play a crucial role as failure of midline fusion results in the loss of this structure as well (Shu *et al.* 2003). By E17 structured midline glial structures such as the the glial wedge, indusium griseum and subcallosal sling, are present. These populations of glia provide pro-growth and targeting signaling such as SEMA3C, FGFR1-3 and Slit-2 necessary for axonal growth and targeting of the callosal axons. Concurrent with midline patterning and fusion, neuronal specification within the neocortex occurs, with a variety of transcription factors (SATB2, Cux2, Limch1) determining the layer fate of neurons destined to be projection neurons in layers II/III, V, and VI (Zhao *et al.* 2011, Niquille *et al.* 2009). Loss of these genes can lead to

a failure of callosal formation. While the corpus callosum is primarily composed of neurons residing in neocortical layers II/III and V, important for anterior callosal development are a group of pioneering axons arise from the cingulate gyrus(Rash *et al.* 2001). While only placental mammals have a corpus callosum and lower organisms lack one, the principle of pioneering axons (particularly across the midline of the left-right axis) still exists. Heat ablation of pioneer axons analogs in zebrafish and grasshoppers prevents the later decussating axons from properly targeting and synapsing with downstream neurons(Sato-Medea *et al.*, 2006). Mouse models have shown that normal development of the corpus callosum relies on a similar "guiding axon" principle to the ones found in lower organisms with essential "pioneer" axons of the cingulate cortex, and that the bulk of axons which form the mature corpus callosum arise primarily from the cortex follow these initial pioneer axons and rely on them for targeting (Piper *et al.* 2009). The importance of these initial crossing axons of the cingulate gyrus appears to be conserved in humans with decreased size of the cingulum bundle observed in patients with ACC correlated with the severity of their agenesis. (Nakata *et al.* 2009, Piper *et al.* 2009) This axon on axon interaction is likely important as neocortical axons later extend into the midline to form the corpus callosum as in mouse models we see interbraiding between the cingulate axons and callosal axons. In the more caudal regions of the cortex, the hippocampal commissure may provide a similar role as a growth substrate and in humans eventually incorporated within the corpus callosum. By E18 the corpus callosum is fully formed, and the full adult range of size occurring at 1 week after birth (Edwards *et al* 2014)

Single Gene Disorders of the Corpus Callosum

Because the formation of the corpus callosum is complex and requires the interplay of multiple molecular and cellular pathways it is not surprising that there are multiple potential points of failure which will lead to dysgenesis of the corpus callosum. Approximately 30-45% of cases of ACC have an identifiable genetic etiology, 20 to 35% the result of mutations in a single gene.

(Schell-Apacik *et al.* 2008; Bedeschi *et al.* 2006). Given our understanding of the underlying biology and development of the corpus callosum from mouse models as well as the neuroanatomical and clinical findings in human patients, we can categorize single gene causes of ACC into the following 5 broad categories. 1) Failure of proliferation of crucial neuronal or glial populations, 2) neuronal migration and/or specification, 3) midline patterning (the glial zipper, glial wedge), 4) axonal growth and/or guidance, or 5) post-guidance development of cortical projection neurons, or some combination of these factors can cause ACC. While some genetic disorders fit very neatly into one category or the other, many of these single genes have multiple functions and inhibit multiple steps of callosal formation. In the following sections I will give a brief overview of a few noteworthy genes and associated syndromes which feature ACC. Mouse models of certain human genes or of ACC will be brought up when relevant

Failure of proliferation of crucial neuronal or glial populations,

The first category of genetic defects is within genes which cause defects in critical neuronal and glial proliferation. While the connection between impairment of neurogenesis and dysgenesis of the corpus callosum may seem straight forward ie, fewer callosal neurons implies fewer axons and therefore agenesis of the corpus callosum, this is not always the case (Noctor *et al.*, 2004a, Noctor *et al.*, 2004b Kowalczyk *et al.*, 2009). For example autosomal recessive primary microcephaly (MCPH) results from decreased neuronal proliferation and fewer neurons but generally does not have an a-colossal phenotype and no change in overall cortical organization. This suggests that just changing the number of cortical neurons is not sufficient to cause agenesis of the corpus callosum. Because radial glia participate in both neurogenesis as well as serving as a scaffold for cortical migration and patterning, mutations in genes which effect radial glia will result in defects in both neuronal specification and migration as well as neuronal proliferation. ACC is in these cases is not found in isolation, a theme that will recur throughout the following sections. Similarly mutations in transcription factors such as PAX6, EMX2, and

SOX2 which drive neuronal maturation from radial glia to intermediate progenitors can lead to mild or more severe callosal hypoplasia. (Graham *et al.* 2003, Englund *et al.* 2005, Sansom *et al.* 2009). Another notable gene implicated in ACC which has known roles in neuronal proliferation is *DISC1*. DISC1 inhibits neuronal progenitor differentiation by inhibiting β-catenin phosphorylation, which causes cell cycle exit and differentiation (Osbun *et al.*, 2011). *DISC1* has been implicated in in the regulation of many other cellular processes from axonal and dendrite out growth and cell to cell adhesion, and mutations in *DISC1* have also been associated with a small number of schizophrenia cases. This overlap of ACC genes with other broader neurodevelopmental as well as neuropsychiatric disease is a recurring association.

Defects in neuronal migration and specification

Single gene defects in neuronal migration and specification often have a degree of overlap with genes involved in neuronal proliferation, as normal corticogenesis is entwined with the specification of cortical layers. As mentioned in the previous segment, genes such as GPSM2, WDR62 and ASPM which cause microcephaly also play a role in the specialization of radial glial microtubules and therefore interfere with the organization of cortical architecture. Mutations in genes known to effect microtubule structure and stabilization (eg. TUBA1A, DCX) severely effect cortical neuronal migration and also result in severe brain malformations such as lissencephaly, periventricular disorders and ACC(Gleeson *et al.* 1998, Deuel *et al.* 2006O'Driscoll *et al.*, 2010, Tischfield *et al.* 2010) . Mutations in the *ARX* gene which is expressed in the forebrain and maintains specific neuronal subtypes and cortical patterning in mammals leads to X-linked lissencephaly with absent corpus callosum and ambigious genitalia (XLAG) which features lissencephaly, disrupted cortical patterning with only 3 layers instead of 6, epilepsy, and complete ACC. (Miura *et al.* 1997). Carrier females can exhibit isolated ACC and impaired cognitive function and epilepsy (Bonneau *et al.*, 2002), suggesting even reduced dosage of *ARX* can disrupt cortical patterning and corpus callosum formation. While cortical

layer identity is usually decided at time of initial division, the neuron must continue to be specified to its layer and to its targets. the upper layer (Layers I-III) specifier *SATB2*, controls the expression of *SKI* a gene deleted in patients with 1p36 deletion syndrome who present with have agenesis of the corpus callosum, suggesting that failure of continued specification of cortical neurons can cause Agenesis. Mouse *Satb2* knockout models also show agenesis of the corpus callosum and show that SATB2 regulates callosal projection neurons bolstering this association. (Alcamo *et al.* 2008, Britanova, *et al.* 2008),

Midline patterning defects

As mentioned in the previous section on normal development of the corpus callosum, the formation of and patterning of the midline is the first and crucial step in the formation of the substrate through which the corpus callosum will eventually form. Dramatic disruption of the midline such as holoprosencephaly, the failure of the embryonic forebrain to divide into two hemispheres caused by mutations to SHH and its receptor PTCH1 Such a dramatic failure and the loss of the midline entirely causes failure of the corpus callosum to form, though this is generally not considered agenesis of the corpus callosum by itself(Robbins *et al.* 2012, Zhang *et al.* 2006,). As mentioned in the previous section, the expression of *Fgf8* in mice is crucial to the induction hemispheric bifurcation. Mutations in Human FGF have been implicated in two syndromes for which ACC has been occasionally reported, Apert syndrome (Wilkie *et al.*, 1995, Slaney *et al.* 1995, Quintero-Revera *et al.* 2006) and Kallmann syndrome (Huffman *et al.* 2004, Dode *et al.*, 2003, McCabe *et al.* 2011).

Research in the past decade has examined a set of ciliopathies and ACC. These ciliopathies are implicated in the normal function of the primary cilia and seem to cooperate with SHH and downstream KIF7 GLI3 and FGF8 signaling. Examples include Joubert, Meckel, Hydrocephhalus, acrocallosal syndrome, and Bardet Biedl (JSRD) syndromes. Mice lacking

RFX3 a ciliogenic transcription factor show an altered corticoseptal boundary and expanded FGF8 expression, furthering reinforcing the centrality of SHH signaling and the development of the normal midline and the formation of the corpus callosum (Benadiba *et al.* 2012).

Defects in Axonal Growth and/or Guidance

Once cortical neurons have migrated to the proper layer, they must then project their axons across the midline to synapse. Callosal guidance is regulated via external guidance cures as well as internal control of the cytoskeleton to facilitate axon lengthening. While multiple mouse models of axonal guidance genes (*Netrin1, Robo1, dcc*) have ACC, they are embryonic lethal in the mouse knockout model and have not been found in any human patients for likely the same reason. The exception to this is mutations in *EFNB1,* the ephrin-B1 gene, which encodes for a type I membrane protein involved in axonal guidance and causes craniofrontonasal syndrome which features ACC. (Wieland 2004, 2005) As previously mentioned in the section on normal callosal development continued axonal growth is also dependent on interactions between axons both within the developing corpus callosum and between the axons earlier decussating axons from the cingulate gyrus and the later crossing axons from the cortex and eventual synapse formation with end targets. Loss of cell adhesion proteins can therefore disrupt these interactions and also cause syndromic ACC. Mutations in *L1CAM,* cause a broad range of X linked disorders referred to as L1 Syndrome including MASA syndrome, CRASH syndrome, X linked complicated ACC and X-linked complicated spastic paraplegia type 1, all of which (Rosenthal *et al.* 1992, Jouet *et al.* 1994, Vos *et al.* 2010, Fransen *et al.*, 1995) feature mental retardation, and hypoplastic corpus callosum, with variations between phenotypes dependent on the region in which the mutation in L1CAM occurs (Vos *et al.* 2010).

Post Guidance development of Cortical projection neurons

Finally, mutations in genes involved in the maturation and survival of callosal neurons can also cause hypoplasia of the corpus callous. These can involve issues with synaptogenesis and synaptic specificity as well as neuronal homeostasis. Homozygous mutations in *SLC12A6* which encodes K-CL Transporter KCC3 (eponym Andermann syndrome) which is essential maintaining neuronal electrical homeostasis causes ACC and has uniquely been associated postnatal degeneration (Howard *et al.* 2002). It has been hypothesized that the loss of KCC3 leads to a failure in survival in early development, and recent studies with conditional knockout of *KCC3* in parvalbumin neurons show a loss of these neuronal populations strengthening the hypothesis that the disease is related to cell survival and development (Ding *et al.* 2014). The Sherr lab has also discovered mutations in a kinesin gene *KIF1A* associated with agenesis of the corpus callosum, microcephaly, cortical visual impairment, optic neuropathy, ataxia, epilepsy and movement disorders, which present with a degenerative neurologic course. Mutations in this gene is thought to show dramatic decreases in gliding velocity of the kinesin, and the degenerative course suggests a function in neuronal survival and development (Esmaeeli Nieh *et al.*, 2015)

ACC is also a feature in certain enzyme deficiencies in cellular metabolism, including pyruvate dehydrogenase deficiency (Patel *et al.* 2012), Smith-Lemli Opitz Syndrome, Fumarase deficiency (Mroch *et al.* 2012, Zulotsuhko *et al.* 2011, Garcia *et al.* 1973, Fierro *et al.* 1977) and desmoseterolisis. The direct causal link between pyruvate dehydrogenase deficiency and agenesis of the corpus callosum, but Desmosterolosis and Smith-Lemli-Opitz syndrome appear to be deficiencies in cholesterol synthesis due to mutations in *DHCR7* and *DHCR24*(Grover *et al.*, 2011, Fitzky *et al.* 1998, Jira *et al.* 2003).

Why study Agenesis of the corpus callosum?

So why study agenesis of the corpus callosum? We see through the study of single gene disorders that these genes cover a wide spectrum disruption often effect multiple brain areas. As mentioned above, ACC rarely occurs in isolation and is usually accompanied by other disorders of brain development such as intellectual disability, epilepsy, language delay and other cortical malformations such as polymicrogyria and white and grey matter heterotopia. Therefore, studying ACC also gives us insight into how the brain responds to developmental perturbations overall, and reveal potential. Previous work such in the identification of ARX gene in the estrogen pathway in patients with syndromic ACC with epilepsy have provided both insight into brain development, elucidation of molecular pathways, and eventually led to potential new inroads for therapy in mouse models and potentially human patients (Sherr at al, 2003, Olivetti *et al.* 2014). Of ACC cases with a presumed genetic cause, only 35% have a causative mutation, highlighting the need for more research into the genetic causes of ACC (Bedeschi *et al.* 2006, Schell-Apacick *et al.* 2008). I will focus on two genes, DDX3X and C12ORF57/Camkinin, whose function in callosal and more broadly brain development was previously unknown, and for which we have been able to provide crucial new insight into both their specific molecular function in this context as well as new knowledge into broader brain and cortical development.

CHAPTER 2: DDX3X

Introduction and Background

From previous reports, it is estimated that between 1-3% of females with unexplained intellectual disability (ID) may have *de novo* nonsense, frameshift, splice site or missense mutations in *DDX3X* (Snijders Blok *et al.,* 2015; Wang *et al.,* 2018) In these publications, approximately 70 individuals have been reported who present with diverse neurologic phenotypes, including microcephaly, corpus callosum hypoplasia, ventricular enlargement, and

epilepsy, which together are identified as the *DDX3X* syndrome*. De novo* mutations in *DDX3X* have also been identified in individuals with autism spectrum disorder (ASD) (Iossifov *et al.*, 2014; RK *et al.*, 2017) and Toriello-Carey syndrome, a causally heterogeneous disorder characterized by severe ID, microcephaly, agenesis of the corpus callosum, post-natal growth defects, and craniofacial abnormalities (Dikow *et al.*, 2017;). In addition to its role in neurodevelopmental disorders, *DDX3X* is recurrently mutated in several cancers, including medulloblastoma and lymphoma (Jiang *et al.*, 2015; Jones *et al.*, 2012; Pugh *et al.*, 2012; Robinson *et al.*, 2012) and in some cases identical residues are mutated in both ID and cancer. Early studies linked missense and nonsense mutations mechanistically by suggesting that *DDX3X* missense mutations may function primarily in a haploinsufficient manner (Snijders Blok *et al.*, 2015). However, to understand the likely pathophysiology, these phenotype/genotype correlations require detailed investigation with a large and fully phenotyped cohort of patients, and in vitro models of DDX3X function.

DDX3X encodes an RNA-binding protein of the DEAD-box family (Sharma and Jankowsky, 2014). While broadly implicated in mRNA metabolism, DDX3X is best characterized as a translational regulator (Lai *et al.*, 2008; Shih *et al.*, 2008). DDX3X is not required for global translation per se, but specifically facilitates translation initiation of mRNAs which contain highly structured 5′ untranslated regions (UTRs) (Chen *et al.*, 2018; Phung *et al.*, 2019). DDX3X is also a component of ribonucleoprotein granules composed of mRNA and protein (mRNPs). This includes neuronal transport granules (Elvira *et al.*, 2006; Kanai *et al.*, 2004) and cytoplasmic stress granules, which are RNA-protein foci induced by cellular stress (Markmiller *et al.*, 2018). DDX3X can regulate the assembly of stress granules (Shih *et al.*, 2012), and overexpression of the wild-type (WT) protein or expression of cancer-associated mutations is sufficient to nucleate stress granules (Lai *et al.*, 2008; Valentin-Vega *et al.*, 2016). RNA-protein granules are a pathological hallmark of many neurodegenerative diseases and an emerging concept is that

disease mutations may act by perturbing the assembly and/or disassembly of RNA-protein granules (Nedelsky and Taylor, 2019). However, it is unknown whether aberrant mRNA metabolism and/or RNA-protein granules are associated with neurodevelopmental pathologies of *DDX3X* syndrome.

In animal models, *Ddx3x* is essential for cell viability and division. *Ddx3x* depletion from mouse zygotes impairs blastocyst divisions and induces apoptosis, while depletion from immortalized cells disrupts chromosome segregation (Li *et al.*, 2014; Pek and Kai, 2011). Likewise, in *Drosophila* germline stem cells, the *DDX3X* ortholog, *Belle,* is required for mitotic progression and survival (Kotov *et al.*, 2016). Germline *Ddx3x* hemizygous male mouse embryos exhibit early post-implantation lethality at embryonic day (E) 6.5 (Chen *et al.*, 2016). Further, epiblast-specific *Ddx3x* hemizygous male embryos show apoptosis, DNA damage and cell cycle arrest, resulting in aberrant neural tube closure and lethality at E11.5. Notably, *Ddx3x* heterozygous female mice have normal viability. *DDX3X* is located in a 735 kb region in Xp11.4 that contains a small cluster of four genes (*CXorf38, MED14, USP9X, DDX3X*) that can escape X inactivation (Carrel and Willard, 2005). However, several studies indicate escape for DDX3X is developmentally regulated, tissue specific, and can be highly variable between cells (Garieri *et al.*, 2018) (Chen *et al.*, 2016).

DDX3X brain malformations overwhelmingly affect the cerebral cortex, and thus are likely rooted in defective development of this structure. Embryonic cortical development relies upon precise generation and migration of both excitatory and inhibitory neurons. Neurogenesis occurs between E11.5 and E18.5 in mice, and between gestation week (GW) 7 and 20 in humans. The main glutamatergic neural precursors are radial glial cells (RGCs), which divide in the ventricular zone (VZ) to produce either neurons or basal progenitors. In mice, the primary basal progenitors are intermediate progenitors (IPs) which generate neurons in the sub-ventricular zone (SVZ). Excitatory neurons are produced in an inside-out fashion, and following their

genesis, migrate into the cortical plate (CP) using the RGC basal process as a scaffold (Taverna *et al.*, 2014). Disorganization of the RGC basal process and/or defective neuronal migration are hypothesized to cause polymicrogyria (PMG) (Jamuar and Walsh, 2015). Likewise, impaired neuronal generation and/or survival can cause microcephaly and are invoked in etiology of ID (Polioudakis *et al.*, 2019). Although DDX3X function in cortical development has yet to be examined, it is essential for neurite outgrowth of cultured rat cortical and hippocampal neurons (Chen *et al.*, 2016). Together with the cell cycle studies highlighted above, this suggests that defects in neural progenitor differentiation or neuronal migration, as well as disrupted formation of the radial glial scaffold could underlie brain malformations associated with *DDX3X* syndrome.

While *DDX3X* mutations have been clearly linked to profound clinical deficits, the developmental and molecular mechanisms, as well as critical genotype-phenotype correlations, remain almost entirely unknown. Here we show that deleterious *DDX3X* variants result in aberrant development of the cerebral cortex in mice and humans. We identify 107 individuals with missense, frameshift, nonsense and splice site *DDX3X* mutations, including 15 recurrently mutated residues and splice sites. 102 of these mutations are in females and not found in either parent (hence *de novo;* two parental pairs were not tested) and three male carriers harbor inherited hemizygous *DDX3X* mutations. Eleven *DDX3X* mutations result in more severe clinical deficits, including PMG and disrupted corpus callosum anatomy, than seen in patients harboring loss-of-function (LoF) mutations. We then use *in vivo* studies in mice to demonstrate that *Ddx3x* depletion impairs neural progenitor function, resulting in reduced neuronal generation in the developing cerebral cortex. Finally, we show that *DDX3X* missense mutations exhibit reduced helicase activity, associated with formation of aberrant RNA-protein granules, and perturbed translation of select targets. Our data demonstrate a consistent correlation between severity of biochemical and cell biological assays, brain imaging and clinical outcomes. This work sheds

light on novel and fundamental developmental and cellular mechanisms that underlie the etiology of *DDX3X* syndrome.

Results

Identification of 107 individuals with *DDX3X* mutations and the associated clinical spectrum

To comprehensively investigate the spectrum of clinical phenotypes associated with *DDX3X* mutations, we identified *de novo* mutations in the *DDX3X* gene in 102 females and three male carriers (Kellaris *et al.*, 2018) with maternally inherited hemizygous *DDX3X* mutations ; two female patients did not have parental testing—with 107 individuals in total--and 11 of these individuals were previously reported **(Figure 2.1)** (Snijders Blok *et al.*, 2015). This cohort was recruited through collaboration with clinical geneticists and neurologists, clinical genetic laboratories, and through the DDX3X family support foundation (DDX3X.org).

To characterize the clinical features of these patients we obtained MRI scans (89 patients) and medical records (106). 53 families were able to complete the Vineland Adaptive Behavior Scales that assessed their child's development in a standardized manner. Two screening tools, the Social Responsiveness Scale-II (49 participants) and the Social Communication Questionnaire (42 participants) were used to assess risk for an ASD diagnosis and risk for social impairment. Within the cohort of 106 patients for which we were able to obtain clinical records, 100% of patients had some neurologic finding reported, with the most common being ID followed by muscle tone abnormalities (91%, 85/93 patients where tone was noted in the records) (Table 2.1). Given that patients are clinically ascertained in this manner the penetrance is not unexpected, but the severity of neurologic and cognitive findings we observed does not automatically follow from this same ascertainment bias. We compared patient scores on the aforementioned standardized tests (Vineland, SRS-II, SCQ) to neurotypical controls. Overall,

patients had a significant deviation in the mean score in all 3 exams (Vineland: 56.4 (15), p<0.001; SRSII 71.6 (12), p<0.001; SCQ 17.5 (7.6), p=0.03; CBC 58 (10), p<0.001) when compared to neurotypical populations (100, <59, <15, 50). Variation between scores on different tests was observed in the same patient, and a degree of variation equal to the variation observed in a control cohort was seen in the *DDX3X* mutation carriers. The scores on the SCQ suggest that 67% (28/42) of the cohort were above the "at risk" threshold for ASD and should be evaluated by a trained clinician to test whether the child's clinical challenges meet criteria for ASD. Seventeen individuals (18%) in the cohort have seizures (ranging from Doose syndrome and infantile spasms to focal partial seizures or generalized absence spells), and 34 participants (38%) have microcephaly (defined as less than or equal to the 3rd percentile). Other less common issues include optic coloboma and strabismus (Table 2.1). In addition to CNS related conditions, cardiac malformations are also present, including ventricular septal defects and atrial septal defects requiring repair (n=13 with 5 requiring surgical repair). This is consistent with a prior case report suggesting that *DDX3X* mutation is associated with Toriello-Carey syndrome (Dikow *et al.*, 2017). Scoliosis was present in 15 participants (16%), which is likely linked to the significant hypotonia and weakness. Three patients were reported to have neuroblastoma, two of which were detected incidentally and all three patients were disease-free at annual follow ups. This observance is consistent with numerous reports indicating that DDX3X is mutated or upregulated in several cancers (Jiang *et al.*, 2015; Jones *et al.*, 2012; Pugh *et al.*, 2012; Robinson *et al.*, 2012). While previous literature on patients with germline *DDX3X* mutations focused primarily on the finding of intellectual and developmental disability (Snijders Blok *et al.*, 2015), these data suggest that the full clinical spectrum found in these patients includes involvement outside the CNS, with significant implications for medical management (Beal *et al.*, 2019).

Location and type of mutation predicts imaging features and clinical outcomes

We sought to determine if the location and type of *DDX3X* mutation found in patients correlated with the severity of their clinical phenotype. We first focused on mutation type, for which there are 57 individuals with missense mutations or in-frame deletions, 38 individuals with nonsense or frameshift mutations (LoF), and 12 patients with splice site mutations **(Figure 2.1)** Patients with missense mutations were significantly more likely to have a severely impaired radiological or clinical phenotype, such as PMG ($p<0.001$) compared to the cohort overall. In parallel, not a single patient with a frameshift or nonsense LoF mutation presented with PMG ($p<0.001$).

The high rate of recurrent mutations led us to ask whether patients with identical mutations present with similar clinical phenotypes. In the cohort we identified 15 nucleotide positions that were repeatedly mutated; and the probability of each of these individual loci having recurrent mutations, given the number of overall mutations, was low and statistically significant for each grouping. This includes six at R488 ($p<1x10^{-15}$, R488C, R488Afs, and four R488H), four patients with mutations at R376 (Arg to Cys, $p<1x10^{-9}$), four patients with mutations at T532M ($p<1x10^{-10}$) three patients with mutations at R326 ($p<1x10^{-7}$), three at I415 ($p<1x10^{-7}$), and two patients each with mutations at the remaining 10 recurrent loci ($p<0.001$).

Of the loci with recurrent mutations, while the numbers were too small to conduct statistical analyses comparing the severity of clinical deficits, qualitative analysis suggests that they result in very similar phenotypes. For example, two of three patients with a T532M mutation had PMG and the third dysgyria. Similarly, all patients with a mutation at residue 415 had PMG (2/3) or dysgyria. Three patients who each had the same *de novo* mutation at R326H exhibited a similarly severe imaging and clinical phenotype, notable for PMG, severe developmental delay and were non-verbal. Conversely, the four patients with the R376C mutation presented with no cortical malformations, a present but thin corpus callosum body and splenium, and a generally less severe clinical presentation. Three out of four patients are speaking in full sentences and

had an average Vineland score of 71. In contrast the average score was 56.4 for the total cohort of 53 patients. Non-neurologic phenotypes can also cluster, as the three patients with mutations at residue I415 had cardiac malformations (ASD, PFO, PDA, PPHN).

Strikingly, of the 11 patients who had PMG, 10 had missense mutations (one had an in-frame single amino acid deletion) with 9 of these mutations found at three recurrent loci (T532, I415, R326). This suggests that these recurrently mutated loci are more commonly associated with PMG ($p=0.01$). PMG patients presented with a more severe anatomic brain phenotype as 7 of 10 (70%) had microcephaly (<3rd percentile, one patient did not have head circumference noted), whereas only 27 of the 80 individuals (34%) without PMG had microcephaly ($p<0.05$). This suggests a potentially mechanistic linkage between microcephaly and PMG in this cohort. This association between missense mutations and PMG suggests that this subset of missense mutations function in a dominant manner, more severe than any of the patients with LoF mutations, none of whom have PMG. Furthermore, 5/13 patients with cardiac findings (two with ASD, one with VSD, one with both a PFO and PDA and one patient with PPHN) also had PMG, disproportionate to the number of PMG patients in the overall cohort ($p<0.05$). PMG patients were also more likely to have partial ACC (27% vs 1% $p<0.05$). Overall, these data suggest that there is an association between certain clinical features and the type of mutation, with a subset of missense mutations being more likely to result in a severe clinical phenotype.

DDX3X missense mutations impair helicase activity that correlates with disease severity

The mouse studies establish essential requirements of *Ddx3x* in cortical development and indicate mechanisms by which *DDX3X* LoF may drive disease etiology. We next turned our attention to investigate the pathogenesis of *DDX3X* missense mutations. These mutations contribute to about half of our clinical cohort and a subset were associated with more severe clinical outcomes than LoF. As *DDX3X* missense mutations fall almost entirely within the two helicase domains, we hypothesized they directly impair DDX3X helicase activity. We further

predicted that if *DDX3X* mutations show impaired helicase activity, there might be a correlation between disease severity and biochemical activity. We therefore measured the ability of purified mutant DDX3 helicase-domain constructs to unwind RNA duplexes (**Figure 2.2A**) (Floor *et al.*, 2016b). We selected recurrent *DDX3X* missense mutations associated with less severe clinical outcomes (R376C, I514T, A233V), severe impairment (R475G), or with severe clinical impairment and PMG (T323I, R326H, I415del, T532M). Duplex unwinding by all mutant proteins was lower than wild-type by varying degrees (**Figure 2.2B**). Notably, there was mild to moderate slowing in the rate of unwinding with mutations found in less severely affected individuals (R376C, I514T, A233V), but complete loss of unwinding activity in all four of the PMG-associated mutations. This indicates that the most severe *DDX3X* missense mutants lack biochemical activity, while less severe missense mutants retain some activity.

To further define the biochemical defect in *DDX3X* missense mutants, we measured v_{max} and K_m for RNA using ATP hydrolysis assays. RNA stimulates ATP hydrolysis by DEAD-box proteins, and thus, changing the RNA concentration in turn, modulates ATP hydrolysis kinetics (Lorsch and Herschlag, 1999). Overall v_{max} and K_m were diminished in *DDX3X* mutants (**Figures 1.2C and D**), with stronger and more consistent effects for v_{max}. We note that it is challenging to accurately fit K_m for the most severely affected mutants as their ATP hydrolysis rates are close to the limit of detection. Taken together, these assays suggest that *DDX3X* missense mutations result in a range of biochemical activity loss, which correlates with clinical disease severity.

Development of high throughput real-time Helicase unwinding assay

While the previously described experiments were capable of producing clear reproducible data, the usage of radioactive isotopes and the manner in which the separation of the helix duplex was measured, manual quantification of phosphoscreen, are not conducive to large scale high throughput applications. As an eventual goal of our investigation into DDX3X involved the

discovery potential treatment for patients with DDX3X mutations, a high throughput method for determining helicase function could prove useful in determining potentially useful compounds in modulating DDX3X activity. We therefore modified a fluorescence based DEAD-box helicase assay originally described by Fraser *et al.* 2019, in which the two strands of the paired 3' and 5' ends of the RNA duplex were labeled with an Alexa546 fluorphore and an IowaBlack quencher respectively. Unwinding the duplex by the DEAD-box helicase leads to a dissociation of the quencher and the fluorophore which then associates with the abundance of complementary DNA bait strands allowing for the uncloaking of the fluorescent signal (Ozes *et al,* 2008)While the original protocol is also not high throughput and described a reaction taking place in a 1 ml cuvette with fluorescence measured serially by insertion of the cuvette into a fluorometer, we miniaturized the experiment so that it could be run in a 20ul volume in a 385 well plate and read using an automated plate reader. Our method allows for a high throughput real time read of the uniwinding activity of DDX3X *in vitro* and is sensitive to changes in concentrations of the protein (**Figure 2.3A**). Furthermore utilizing this method was able to reproduce the loss of function in the mutant DDX3X proteins found in human patients as well and that the milder mutation (R376C) would increase unwinding activity in response to increased concentration from 1 uM to 4 uM, the more severe PMG associated mutations (T323I, and R326H) had no response to changes in protein concentration in the assay, showing the ability even at a limited scale of this higher throughput method for more readily testing various assay conditions(**Figures 1.3C and D**). Further steps will be to test both inhibitors as well as a library of compounds to find potential positive modulators which could prove useful to future.

Discussion

DDX3X has recently been recognized as a frequently mutated gene in both ID and cancer, yet the mechanism by which *DDX3X* mutations impair brain development have not been defined. Here, we report the largest cohort of patients with *de novo* mutations in *DDX3X* (n=107) to date,

highlighting corpus callosum abnormalities and PMG as two major brain anatomic phenotypes characteristic of *DDX3X* syndrome, with PMG strongly linked to missense mutations and to significant clinical impairment. Further, using *in vivo* mouse studies, we link these phenotypes to developmental mechanisms, showing that *DDX3X* is essential for proper cortical development by controlling neural progenitor differentiation. Finally, using biochemical and cell biological assays, we show that *DDX3X* missense mutations disrupt helicase activity, which is associated with altered RNA-protein granule dynamics and RNA metabolism. The severity of these biochemical and cellular impairments correlates closely with clinical severity, supporting the hypothesis that a subset of missense mutations function in a dominant negative manner, a novel and important finding for understanding DDX3X's role in brain development. Altogether, our study uncovers new cellular and molecular mechanisms by which *DDX3X* mutations induce severe cortical malformations in humans, and broadly implicates new pathogenic etiologies of neurodevelopmental disorders.

Location and type of mutation predict *DDX3X* clinical phenotype

In this study, we identify and characterize phenotypes for 107 patients, significantly extending our understanding of clinical outcomes associated with *DDX3X* mutations. Detailed analysis of our expanded cohort reveals the same recurrent *de novo* mutations in unrelated individuals result in markedly similar clinical phenotypes. Three pairs of patients (9 total) with PMG have mutations at recurrent amino acids, R326, I415, and T532. Indeed, the R326 mutation was also reported previously together with PMG (Snijders Blok *et al.*, 2015). Within our cohort, we recognized five new PMG mutations (V206M, T323I, I415F, I415del, T532M). All of the patients with mutations at these amino acids had a more severe cerebral anatomic phenotype, including complete or partial absence of the corpus callosum. The correlation with PMG is important as these patients also tended to have more complicated clinical presentations, including epilepsy, autism spectrum disorder, severe intellectual disability, and structural cardiovascular

malformations than patients without PMG. Of the eleven patients with PMG, ten were found to have missense mutations and one had a three-nucleotide deletion, which is predicted to result in a single amino acid deletion. This striking association between PMG and missense mutations supports the hypothesis that certain missense mutations may generate a more severe "dominant negative" phenotype. In contrast to the association of some missense mutations with more severe disease phenotypes, the most common recurrent mutation, R376C, showed a milder phenotype overall, with only 1 out of 4 patients being nonverbal past the age of 8, and all were normocephalic.

In contrast, none of the 39 patients with LoF mutations had PMG. Instead these patients with LoF mutations exhibited a milder spectrum of clinical phenotypes, including preservation of the ability to walk and talk. This degree of genotype-phenotype association was not evident in the first reported cohort of *DDX3X* patients (Snijders Blok *et al.*, 2015) or in subsequent cohorts (Wang *et al.*, 2018), perhaps due to a smaller sample size.

RNA metabolism is severely impaired by *DDX3X* missense mutants

Our data pinpoint defective RNA metabolism as an underlying mechanism by which *DDX3X* missense mutations impact progenitors and neurons. We show that *DDX3X* missense mutants have reduced helicase activity, predicted to impair release of the protein from RNA. Further we show that *DDX3X* missense mutants cause aberrant RNA-protein granule formation, with features resembling stress granules. As DDX3X normally forms functional trimers (Valentin-Vega *et al.*, 2016), we predict that missense mutants with impaired helicase activity act as dominant negatives. As a result, by failing to release from RNA, mutant DDX3X may aberrantly sequester both RNA and RNA binding proteins within the cell.. Strikingly, *DDX3X* mutations associated with the most severe clinical outcomes induce the strongest cell biological and biochemical phenotypes. In contrast, mild mutants which still maintain some helicase activity behave similar to loss-of-function, and do not induce aberrant granules. Altogether this provides

a molecular explanation for observing more severe clinical phenotypes with missense mutations compared to carriers of nonsense and frameshift (presumed LoF) mutations.

How might these RNA metabolism defects ultimately influence gene expression in progenitors and neurons? While global translation was unaffected by *Ddx3x* LoF or expression of missense mutations, DDX3X missense mutants did alter translation of specific targets. This suggests that DDX3X missense mutants may affect neurogenesis by disrupting translation of specific targets, including those which promote neuronal generation. These questions should be addressed in the future with comprehensive genomic studies of both LoF and missense variants.

In the current study we employed exogenous expression to assess the cell biological consequences of *DDX3X* missense mutations. This approach has been widely used for investigations of RNA binding proteins, including DDX3X, in stress granules and translation (Valentin-Vega *et al.*, 2016; Lessel *et al.*, AmJHum Genet, 2018; Yasuda *et al.*) For our experiments we carefully controlled for overexpression by titrating down levels of transfected DNA, and by comparing all results using wild-type and missense constructs expressed at similar levels. Using this paradigm, quantifiable and reproducible differences were detected between WT and missense DDX3X, expressed at similar levels. However, many RNA binding proteins exhibit exquisite dosage sensitivity, where either too much or too little can cause cellular dysfunction (Mittal *et al.*, 2009). Thus going forward it will be valuable to develop new approaches to assess the consequences of endogenously expressed *DDX3X* missense mutations.

High Throughput Helicase Fluorescent assays show promise for testing large

While other helicase assays utilizing both fluorescent and radioactively labeled RNA duplexes have previously been published our work and development of a fluorescent real time helicase assay represents the first published protocol for high throughput helicase assay (Floor *et al.*

2012, Ozes *et al.* 2008). This high throughput method would give us the ability to screen large small molecule libraries for candidate compounds that can positively or negatively modulate DDX3X. While DDX3X has relatively promiscuous binding and no consensus sequence, high throughput methods will also allow for determining *in vitro* any potential changes to sequence specificity via randomized dimers.

Materials and methods

Data Reporting

No statistical methods were used to predetermine sample size for this study. Recruitment for this study was not blinded.

Sample

This study includes data from 107 participants from a network of seven clinical sites. Data collection sites had study protocols approved by their Institutional Review Boards (IRB), and all enrolled subjects had informed consent provided by parent/guardian.

Data Collection Methods

The majority of mutations were identified through clinical whole exome sequencing either at referring and participating clinical centers or through the clinical genetic laboratories: GeneDx, Baylor, or BGI-Xome. Three patients (2839-0, 2839-3 and 2897-0) were ascertained as part of a larger study of genetic causes for Dandy-Walker malformation. Exome sequencing of 2839-0 and 2897-0 and their parents was performed as described (Van De Weghe *et al.*, 2017); 2839-3 is the identical twin of 2839-0 and Sanger sequencing confirmed she shared the mutation identified by exome sequencing in her sister. Genetic mutation data were obtained for all 107 participants. All clinical features and findings were defined by the medical records obtained from

participants or from the completion of standardized behavioral and development measures. Thus, the parents of the probands were issued the following neuropsychological questionnaires according to their child's age: Vineland Adaptive Behavior Scales, Second Edition (Vineland-II), Child Behavior Checklist (CBCL), Social Communication Questionnaire (SCQ) and Social Responsiveness Scale, Second Edition (SRS-2). 53 of the study's 107 participants completed at least one neuropsychological questionnaire. Comparison of population means for behavioral scales were performed using a Wilcoxon test. One patient had a low quality MRI scan and it could not be determined whether PMG was present or absent with the current data; therefore 106/107 patients are represented in the clinical data table.

MRI Review

This study includes MRI scans from 89 participants. 9 patients in the cohort did not have MRI scans in their records and 8 MRIs could not be obtained. All scans were initially reviewed locally by a radiologist for findings that, if present, were communicated to the participant and noted in the patient chart. DiCOM files of high quality MRI scans were then transmitted and neuroradiologic findings were noted in a standardized assessment of developmental features as previously utilized by our group (Hetts *et al.*, 2006). All MRI findings were reviewed by a board certified pediatric neuroradiologist at UCSF blinded to genetic status as part of a larger more general review of potential agenesis of the corpus callosum cases.

Statistical analysis of clinical data

Comparisons of various frequencies between the groups were performed based on Fisher's exact test. One-sample tests of frequencies of the observed mutations were performed using Binomial test. Comparisons of continuous measures were performed using Mann-Whitney U-Test.

Purification of recombinant DDX3X WT and mutant

Plasmids encoding amino acid residues #132-607 were transformed into competent *E.coli* BL21-star cells, lysed by sonication in lysis buffer (0.5 M NaCl, 0.5% NP40, 10 mM Imidazole, 20 mM HEPES pH 7.5) and bound to nickel beads, as described (Floor *et al.*, 2016b). Beads were washed with low salt (0.5M NaCl 20 mM Imidazole, 20 mM HEPES) and high salt wash buffers (1 M NaCl, 20 mM Imidazole, 20 mM HEPES pH 7.5) and eluted (0.5 M NaCl, 0.25 M imidazole, 100 mM Na_2SO_4, 9.25 mM NaH_2PO_4, 40.5 mM Na_2HPO_4). The 6xHis-MBP tag was cleaved overnight by *tev* protease at a 1:40 tev:protein ratio (w/w), and then dialyzed into ion exchange low salt buffer (200 mM NaCl, 20 mM HEPES ph7, 10% Glycerol, 0.5 mM TCEP). The sample was loaded onto a GE HiTrap heparin column (GE, 17-0406-01), eluted at 25% ion exchange high salt buffer (1 M NaCl, 20 mM HEPES pH 7, 10% Glycerol, 0.5 mM TCEP) and applied to Superdex 75 column (GE 17-0771-01) equilibrated in 500 mM NaCl, 10% Glycerol, 20 mM HEPES pH 7.5 and 0.5 mM TCEP. Peak fractions were collected, concentrated to ~50 µM, and then supplemented with 20% glycerol, diluted to 30 µM, and flash frozen in liquid nitrogen. Sample of the collected protein was run on a SDS-PAGE gel and stained with Coomassie to confirm protein purity and size.

Radiolabelling and formation of RNA Duplex

Two complementary RNA molecules were synthesized by IDT:
“5’ duplex” (5’-AGCACCGUAAGAGC-3’) and “3’ overhang (5’GCGUCUUUACGGUGCUUAAAACAAAACAAAACAAAACAAAA-3’). 5’ duplex RNA was labeled with ^{32}P using T4 PNK (NEB, M0201S) for one hour at which point stop buffer was added to terminate the reaction. Labeled RNA was run on a 15% DNA denaturing gel, imaged on a phosphorscreen, and then bands were excised and RNA eluted overnight in 600 µL elution

buffer (300 mM NaOAc pH 5.2, 1 mM EDTA, 0.5% SDS). Eluted RNA was then precipitated using 750 µL of 100% ethanol and immersed in dry ice for 1 hour 30 minutes and then resuspended in 20 µL DEPC H_2O to > 200k cpm. RNA duplex was created by annealing 3 µL of 100 µM 3' overhang RNA to 2.5 µL 5' duplex of duplex RNA, heated to 95°C for 1 minute and allowed to cool to 30°C before purifying on a 15% native gel run at 8 watts.

Duplex Unwinding Assays

This protocol was modified from (Jankowsky and Putnam, 2010). Radiolabeled, purified duplex RNA was diluted to ~333 cpm, and protein was diluted to 10 µM concentration. Reaction was run in 30 µL in reaction buffer (40 mM Tris-HCl pH 8, 5mM $MgCl_2$, 0.1% IGEPAL, 20 mM DTT) with 3 µL of diluted RNA and 1 µL of 10 µM protein. 3 µL of 20 mM ATP:$MgCl_2$ was added to initiate the reaction. At each time point 3 µL of reaction mix is removed and quenched in 3 µL of stop buffer (50 mM EDTA, 1% SDS, 0.1% Bromophenol blue, 0.1% Xylene cyanol, 20% glycerol). Reaction time points are then run on a 15% native polyacrylamide gel, at 5 watts for 30 minutes at 4°C. Gel is dried and imaged on a phospho-screen and quantified using ImageQuant software.

ATP-ase activity Assay

The ATPase activity assay was performed with protein constructs previously purified and in the enzyme reaction buffer used the duplex unwinding assay reaction buffer, as described in Floor and Barkovich (Floor *et al.*, 2016a). 100 µL of reaction master mix was made containing 3 µL of 10 µM DDX3X protein, 10 µL of 10x reaction buffer (400 mM Tris-HCl pH 8, 50mM $MgCl_2$, 1% IGEPAL, 200 mM DTT) and 26.9 µL of DEPC H_2O. 2 µL of single stranded RNA was added to each 7 µL to create a dilution series of 0 µM, 0.625 µM, 1.25 µM, 2.5 µM, 5 µM, 10 µM, 20 µM and 40 µM. The single-stranded RNA was transcribed and gel purified, with sequence GGAAUCUCGCUCAUGGUCUCUCUCUCUCUCUCUCUCUCU. Radioactive ATP-(^{32}P)

(Perkin Elmer) was diluted to 666 µCi/uL. 1 µL of ATP at varying concentrations was added to initiate each reaction. At each time point 1 µL were spotted and quenched on PEI cellulose thin layer chromatography plates. Chromotography plates were run in a buffer of 0.5 M LiCl and 0.5 M Formic acid. Plates were then exposed to a GE Phosphoscreen for 1.5 hours and then imaged on a GE Typhoon imager.

Fluorescent unwinding Assay

Two complementary RNA molecules were synthesized by IDT:
"5' duplex" (5'-AGCACCGUAAGAGC-3') conjugated on the 5' prime end an Alexa 568 fluorphore and "3' overhang (5'GCGUCUUUACGGUGCUUAAAACAAAACAAAACAAAACAAAA-3') conjugated to the 3' end to an IOWA Black quenching molecule. Duplex annealing was performed according to the protocol listed out in Ozes *et al.* 2008. Unwinding was performed in a 2ul 1x helicase reaction buffer buffer (40 mM Tris-HCl pH 8, 5mM $MgCl_2$, 0.1% IGEPAL, 20 mM DTT) with DDX3X purified as listed above. Reactions were initiated with the addition of 1 ul of 20 mM ATP/$MgCl_2$ and were read on a TECAN spark with a filter set set for Texas Red.

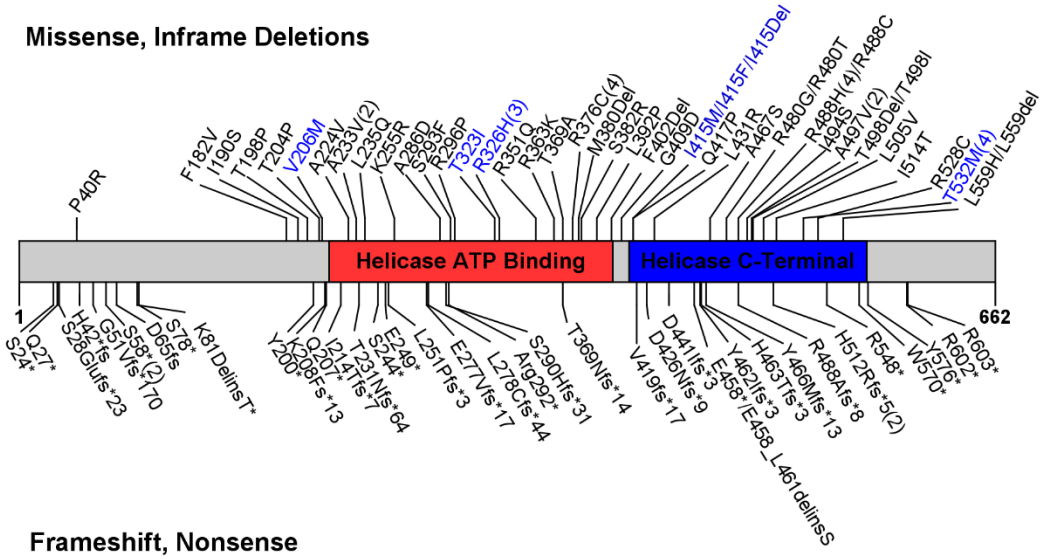

Figure 2.1 Mutations in DDX3X patients: A, Missense and in frame deletions are annotated on top while frameshift and nonsense mutations which likely cause early termination are annotated on the bottom. Mutations found in patients with polymicrogyria are displayed in blue, ten of eleven of which are missense mutations, and one is an in-frame deletion (I415Del). Recurrent mutations are indicated by numbers in the parentheses. Overall, mutations are enriched in the helicase domains at a rate higher than random chance ($p<0.0001$). Not shown are splice site mutations, found at G51, G89, K288 and A499 as the change to the protein sequence could not be reliably predicted.

Table 2.1: Clinical and Imaging findings in DDX3X patients

Imaging Findings	Non-PMG Individuals	PMG Individuals	Combined Total
Corpus Callosum Type			
Complete ACC	0/54 (0%)	1/10 (10%)	1/64 (2%)
Partial ACC	0/54 (0%)	3/10 (30%)	3/64 (5%)
Diffusely thin	20/54 (37%)	0/10 (0%)	20/64 (37%)
Thin posteriorly	23/54 (43%)	6/10 (60%)	29/64 (45%)
Thick	4/54 (7%)	0/10 (0%)	4/64 (6%)
Short	5/54 (9%)	0/10 (0%)	5/64 (8%)
Normal	2/54 (4%)	0/10 (0%)	2/64 (3%)
Ventricles			
Enlarged	**8/54 (15%)***	**6/10 (60%)***	**14/64 (22%)**
Key-hole shaped temporal horns	39/54 (72%)	6/10 (60%)	45/64 (70%)
Colpocephaly	1/54 (2%)	2/10 (20%)	3/64 (8%)
Other			
Small anterior commissure	4/54 (7%)	0/10 (0%)	4/64 (6%)
Small pons	2/54 (4%)	3/10 (30%)	5/64 (8%)
Small inferior vermis	4/54 (7%)	3/10 (30%)	7/64 (11%)
Decreased white matter volume, (cortical)	**19/54 (35%)***	**7/10 (70%)***	**26/64 (41%)**
Decreased cingulum bundle volume	13/54 (24%)	1/10 (10%)	14/64 (22%)

	Non-PMG Individuals	PMG-spectrum Individuals	Combined Total
Neurologic			
ID/DD	95/95 (100%)	11/11 (100%)	106/106 (100%)
Nonverbal (in individuals above 5 years old)	32/68 (47%)	6/7 (86%)	38/75 (51%)
Seizures	15/83 (18%)	2/10 (20%)	17/93 (18%)
Microcephaly (≤3rd percentile)	**27/80 (34%)**	**7/10 (70%)**	34/90 (38%)
Hypotonia	**52/82 (63%)**	**2/11 (18%)**	54/93 (58%)
Hypertonia/Spasticity	3/82 (4%)	2/11 (18%)	5/93 (5%)
Mixed Hypo and Hypertonia	**24/82 (29%)**	**7/11 (64%)**	31/93 (33%)
Ophthalmologic			
Coloboma	2/82 (2%)	2/10 (20%)	4/92 (4%)
Strabismus	22/82 (27%)	3/10 (30%)	25/92 (27%)
Congenital Cardiac Defects	**7/80 (9%)**	**5/10 (50%)**	12/90 (13%)
Other Abnormalities			
Precocious Puberty	9/84 (11%)	2/10 (20%)	11/94 (12%)
Scoliosis	12/84 (14%)	3/10 (30%)	15/94 (16%)

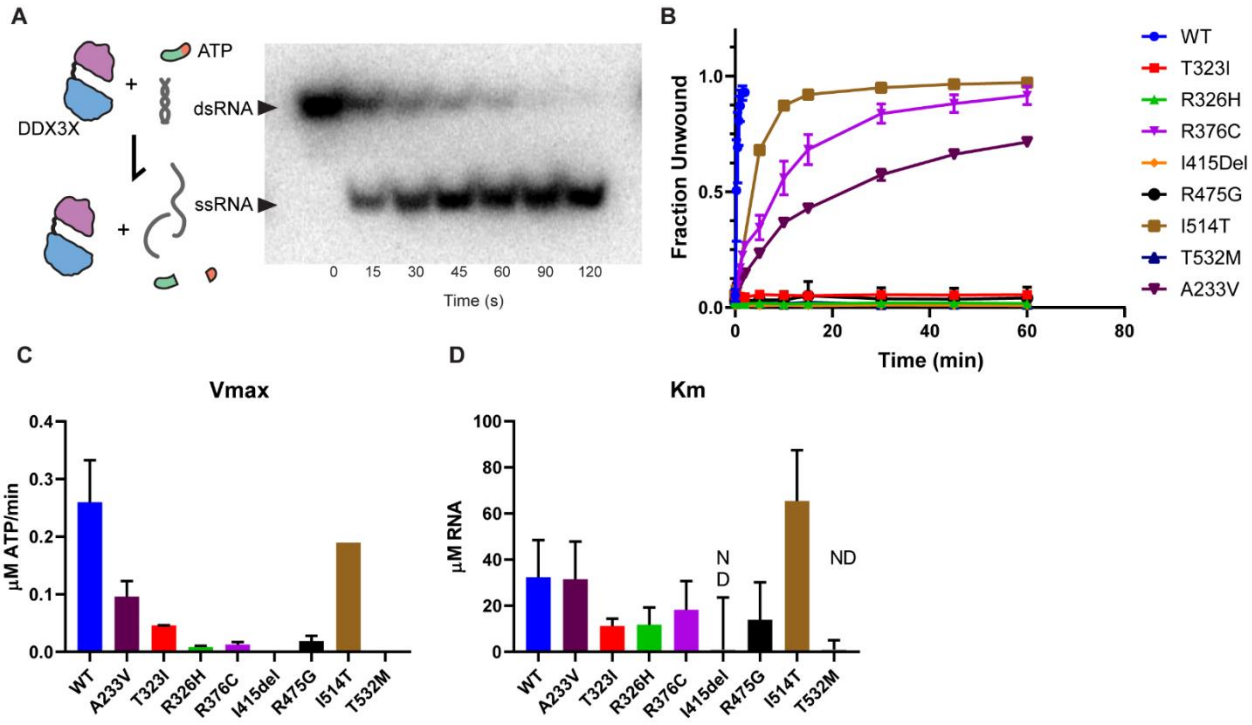

Figure 2.2 *DDX3X* missense mutants exhibit disrupted helicase activity

A, Left, Diagram of DDX3 activity tested in this assay. ATP is necessary for the initial binding of RNA, however ATP hydrolysis is not necessary for RNA unwinding but is required for release of the RNA from the protein complex. Right, blot of unwinding assay. DDX3 constructs were incubated with radioactively labeled RNA duplex and ATP, and aliquots at indicated time points were run on a non-denaturing gel (right). dsRNA runs more slowly than ssRNA, allowing percentage unwound to be quantified by band intensity. B, Unwinding assay for tested mutations in the first and second helicase domains WT, A233V, T323I, R326H, R376C, I415del, R475G, I514T, and T532, All mutants showed a decreased unwinding activity when compared to wild type (Far left). PMG mutants showed no unwinding activity while mutants found in patients with less severe clinical phenotypes (R376C, I514T, A233V) had less impaired unwinding. C, All mutants showed reduced Vmax when compared to the wild type. Two mutants (I415Del, T532M), both PMG mutants, had no detectable activity. D, Km for DDX3X mutants. I415del and T532M had unwinding curves which did not vary within the range of tested RNA concentrations (0-40 uM) so that Km could not be reasonably determined (n.d.). Majority of mutants had lower Km (indicating higher affinity for RNA) than the wild type with the exception of I514T.

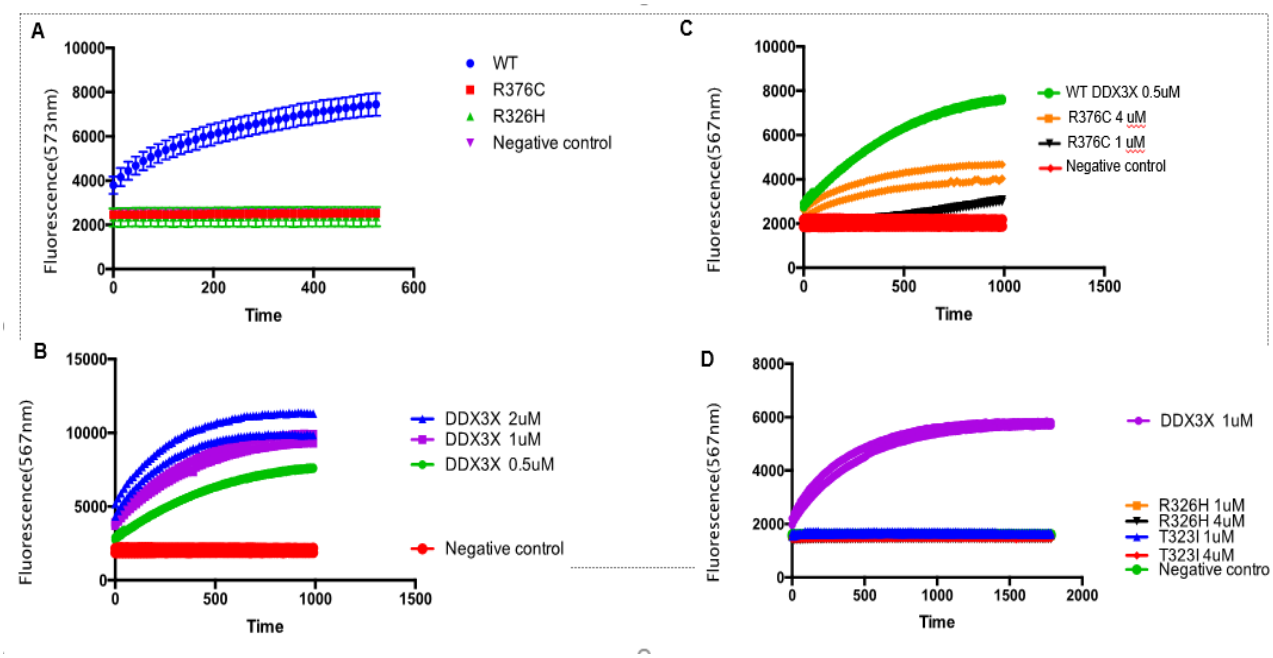

Figure 2.3 Fluorescent DDX3X Unwinding Assay is sensitive to concentration of WT DDX3X and severity of mutant DDX3X

A) Wildtype DDX3X (Blue) shows robust unwinding activity in at 1uM concentration when compared to constructs containing mutants found in the patient cohort R376C (red) and R326H (green) which show no unwinding activity at 7 minutes. B) Wild type DDX3X in the fluorescent assay unwinds at increasing rates as concentration of protein is increased from 0.5 uM (green) to 1 uM (purple) to 2 uM (blue). C) varying concentration DDX3X with the milder R376C shows that increased concentration from 4 uM to 1 uM leads to an increased rate of unwinding, but not at the level of WT at 0.5 uM. In contrast D) mutations found in patients with polymicrogyria show no change even with the same increased concentration of protein, suggesting that this assay has the discriminative ability between severe and milder mutations similar to the radioactive assay described in Figure 2.2.

CHAPTER 3: C12ORF57/Camkinin

Background and Introduction

Recently several groups along with our own have described homozygous loss of function mutations in *C12ORF57* in predominantly Middle Eastern Arab populations which result in Temtamy syndrome (TEMTYS) (OMIM:218340) characterized by dysgenesis of the corpus callosum (both smaller and larger than normal), medically refractory epilepsy, severe intellectual disability, optic coloboma and autism (Zahrani *et al* 2013, Akizu *et al* 2013, Alrakaf *et al* 2018). The vast majority of reported mutations (80.4%) are found in the start codon (c.1A>G, p. 1M>V) suggesting a loss of function mutation with previous data suggesting a dramatic loss of expression (Akizu *et al* 2013). Only one missense mutation (c.t152a, p.L51Q) reported, with the remaining 10% of reported mutations in patients with both alleles affected consisting of splice site mutations. (**Figure 3.1b**) (Alrakaf *et al* 2018) While initial reports of TEMTYS characterized it as an extremely rare disease with a dozen affected individuals and 5 families, this number has since grown to 54 total published individuals in well over a dozen families with a whole exome project performed on 1000 patients with intellectual disability (ID) performed in Saudi Arabia suggests that 1.5% of all hereditary cases of intellectual disability in Middle Eastern Arab populations may be attributed to the c.1A>G homozygous mutations in *C12ORF57* alone (Monies *et al* 2017). This suggests that mutations in C12ORF57 may be of comparable frequency to more well established causes of intellectual disability such as Fragile X in certain populations (Akizu *et al* 2013, Alrakaf *et al* 2018) .

The potential prevalence and severity of the clinical phenotype suggesting that C12ORF57 has a crucial role in normal brain and corpus callosum development stands in contrast to what little is known of the protein. *C12ORF57* is a three exon gene encoding a 127 amino acid protein (C10/C12ORF57) which has a high level of conservation in other mammals from Mus *musculus*

(GRCC10, 98% amino acid identity) to zebrafish (C10, 72% amino acid identity) (**Figure 3.1a**)(Akizu *et al* 2013). However, despite this high level of conservation, protein BLAST of C12ORF57 returns no homologs among known human proteins, and the primary sequence contains no known protein domains. This lack of homology has made previous attempts to ascertain the molecular function of C12ORF57 difficult, and even the most basic questions regarding C12ORF57 remained unanswered: Where is it expressed in the developing brain? What is its biochemical function and in what molecular and biologic pathways does it function? How does it contribute to the human disease phenotype?

In this study we determine that loss of the C12ORF57 murine ortholog *Grcc10* demonstrates phenotypes similar to those found in human patients and is expressed in regions crucial to mouse brain development. We provide for the first time via a combination of biochemistry, cell biology and electrophysiology a role for C12ORF57 in enhancing CAMK4/CREB signaling, and through this neuronal homeostasis of excitatory synapses both in primary neuronal culture and *in situ*.

Results

Grcc10 -/- mutant mice have features similar to patients with homozygous inactivation of C12ORF57

Due to the high level of conservation between C12ORF57 and its mouse ortholog (Grcc10, 98% amino acid identity), we hypothesized that generating a mouse model of C12ORF57 would be a productive approach to study the function of this novel protein. There have been no vertebrate models of C12ORF57. Because the most common mutation in human patients is c.1A>G, this missense mutation, which previous work has shown to eliminate overall protein expression (Akizu *et al* 2013) we obtained mutant mice with constitutively inactivation of Grcc10 from

Jackson lab (Grcc10<tm1.1(KOMP)Vlcg>), generated with a lacZ cassette and complete deletion of exon 2 and portions of Exon 1 and 3. Western blot analysis using affinity purified rabbit anti-sera to Grcc10 confirmed loss of Grcc10 protein expression in the brains of KO mice, and the same antisera detected a 13 kD protein in wild type (WT) mouse brain lysates confirming knockout of the protein. We noted a high level of preweaning mortality in the *Grcc10 -/-* mice (**Figure 3.2A)** a finding that was corroborated by early data from the MGI, with *Grcc10 -/-* displaying a failure to thrive compared to their littermates **(Figure 3.2B).** This high level of preweaning and perinatal mortality in conjunction with our data on the expression of *Grcc10-/-* lead us to believe that whatever pathways implicated in *Grcc10* function were present would likely be present and observable at P0 and in the postnatal period. *Grcc10-/-* mice that survived the perinatal period showed failure to thrive compared to their littermates with P21 mice having only 25% of the mass of their wildtype and heterozygous littermates **(Figure 3.2B).** P0 *Grcc10 -/-* mice had shortened, (792+/-95.9 um vs 958.2+/-61.2 um) as well as decreased cross sectional area of the corpus (154859+/-12087.8 um^2 vs 200123+/-20676.8um^2) compared to WT and heterozygous *Grcc10+/-* mice (**Figure 3.2 C-E).** In patients who all shared the same homozygous C12ORF57 mutation we previously observed a range of corpus callosum dysgenesis from partial to complete absence of the corpus callosum, suggesting that other genetic modifiers may also influence the phenotype(Zahrani *et al* 2013, Akizu *et al* 2013, Alrakaf *et al* 2018)

Seizures are frequently observed in patients with biallelc inactivation of C12ORF57 (73% of patients in a meta-analysis of multiple cohorts (Alrakaf *et al* 2018) By inference we sought to determine if there was increased seizure susceptibility in *Grcc10-/-* mice. We observed behavior consistent with spontaneous seizures in *Grcc10 -/-* mice, but not in WT mice*Grcc10 -/-* mice were too runted to implant surface electrodes. We therefore tested seizure susceptibility directly by measuring Racine seizure scales (Racine, 1962) after injection of the proconvulsant

glutamate agonist kainic acid. 20 µg/kg kainic acid was injected intraperitoneally into WT, *Grcc10 +/-,* and *Grcc10 -/-* mice. These mice were then observed for the time to onset of behavioral Racine stages to measure seizure progression.(Sharma *et al* 2018) (McKhann *et al* 2003) We noted an increased sensitivity to kainic acid administration for *Grcc10 -/-* mice vs. WT counterparts as measured by the time to arrive at each Racine stage **(Figure 3.2F).**

These data present a mammalian model for Temtamy syndrome which shares many key features of the disorder, and suggests a similar function in mouse and human brains for the protein.

Grcc10 **is expressed throughout the developing and adult mouse brain**

Given the early developmental phenotype for *Grcc10-/-* mice and for patients, we hypothesized that *C12ORF57/Grcc10* is expressed at a high level in the developing cerebral cortex. Data are available for adult mice (P56) from the mouse Allen Brain Atlas, showing broad-based expression in the adult brain, in the cerebral cortex, basal ganglia, hippocampus and cerebellum. To assess developmental expression, we conducted ISH (in situ hybridization) using a full length cRNA probe against the *Grcc10* mRNA targeting the sequence utilized by the Allen Brain Atlas. Our *in situ* hybridization data shows that *Grcc10* is expressed throughout the developing brain from embryonic day 15 and through the post natal (P10) period as well. This analysis showed that *Grcc10* expression was detected at the ventricular zone, glial wedge, and cortical plate at E15. In addition to the regions as seen at E15, the expression of *Grcc10* was observed at hippocampus, cingulate cortex, and indusium griseum at E18. The expression of *Grcc10* persisted in those regions for P0 and P10. we see the highest level of expression in the early postnatal and late embryonic period **(Figure 3.3).** The expression pattern in the cortical plate is and hippocampus especially at E18 and P10 is consistent with a neuronal phenotype. Previous genes implicated in disorders human corpus callosum and intellectual

disability have shown a disrupted neuronal outgrowth phenotype *in vitro* and *in situ*, and neuronal proliferation and layer specification so we sought to determine if there were any similar changes in mouse brains.(Fame *et al* 2016, Gennarino *et al* 2018, Srivastava *et al* 2012) We find that in P0 Mice, at time of birth, the overall cortical area and length are unchanged between *Grcc10 -/-* mice compared to *Grcc10 +/+* and *Grcc10+/-* mice. Staining of both upper and lower level cortical layers(SATB2, CTIP2) shows no change in overall neuronal number (p=.452,n=6) (**Figure 3.4)** in either layer between *Grcc10+/+* and -/- P0 mice, suggesting that loss of *Grcc10* does not grossly impair overall corticogenesis, or the layer specificity of the neurons

Loss of C12ORF57 increases basal neuronal excitability in hippocampal neurons

Given the frequency of epilepsy in C12ORF57 patients the increased sensitivity to kainic acid in *Grcc10-/-* mice, and the expression of C12ORF57 in neurons we sought to elucidate the electrophysiologic profile of hippocampal neurons in these mice. We treated DIV7 neurons overnight with KCl, which in wildtype neurons increases neuronal branching in an activity dependent manner, caused a slight decrease in overall neuronal branching in *Grcc10-/-* neurons which initially had slightly higher overall branching than their WT counterparts **(Figure 3.5 A-C).** This suggest an activity dependent mechanism for C12ORF57 which is consistent with our observations of increased epilepsy sensitivity in the knockout mice and potentially suggests a baseline increased sensitivity in KO neurons and an inability to tolerate increased excitation. We measured mEPSCs from cultured E18 DIV14 hippocampal neurons from *Grcc10+/+ , +/-* and -/- mice. We saw a profound increase in both mean amplitude of mEPSC (10 pA vs 18pA p<.0001) as well as frequency (3 events/sec vs 7 events/sec) in *Grcc10 -/-*mice in primary dissociated cultures compared to WT . Heterozygote mice showed a statistically significant but considerably smaller change in amplitude (11.3 pA vs 18 pa, P<.001) and frequency when compared to the wildtype. These data are consistent with our observation of kainic acid sensitivity in our *Grcc10-/-* mouse model **(Figure 3.2F)** These peaks were sharp and consistent

with AMPA current. We see an increase in the number in GluA2 and VGLUT2 positive puncta in E18 DIV14 *Grcc10 -/-* hippocampal neurons compared to WT neurons **(Figure 2.5 G-H).** These data suggest that *C12ORF57/Grcc10* play a critical role in maintaining normal excitatory neuronal homeostasis and whose loss results in an increase in overall excitatory synapses specifically through the GluA2/AMPA current.

C12ORF57 is a novel protein and a regulatory binding partner for CAMK4

Our functional studies have shown a dramatic change in both cellular and animal models in response to loss of C12ORF57 reflective of the phenotype seen in human patients. The exact biochemical function of C12ORF57 remains a mystery. To identify further interrogate the function of C12ORF57 in the developing and post-natal CNS, we conducted two independent unbiased Yeast 2 Hybrid (Y2H) screens with a library composed of a commercial normalized Mate and Plate cDNA screen from a normalized mix of BALBC mouse brain. Each screen resulted in a single positive clone that encoded the same Calcium/calmodulin associated kinase 4 from a domain spanning residues 300-469. We tested whether an interaction occurs between these two proteins in vivo by conducting a co-immunoprecipitation experiment, using separately antibody to Grcc10 and then antibody to CamkIV, strengthening the evidence linking these proteins brain (**Figure 2.6A**). Calcium calmodulin associated Kinase IV (CAMK4), is a member of the CAMK family which is activated by neuronal activation and the influx of calcium into the neuron leading to binding of calmodulin (AA residues 322-341) followed by the phosphorylation at the key residue Thr200 (*Homo Sapiens*)/ Thr196 (*Mus musculus*). Phosphorylation at this primary site causes a change in protein confirmation moving an autoinhibitory domain loop (residues 305-321) out of steric hindrance of the kinase domain (Chatila *et al* 1996) (**Figure 3.6B**). This change in conformation initiates translocation to the nucleus and activation of its kinase activity(Tokumitsu *et al* 1994, Enslen *et al* 1996). Binding of protein phosphatases (PP1, PP2) to this autoinhibitory domain leads to dephosphorylation of Thr200 and the deactivation of

the protein (Kashara *et al* 1999). Given that both the calmodulin and autoinhibitory binding domains are essential to CAMK4 regulation, we sought to test whether one or both of these domains contributed to this intramolecular interaction. We created two CAMK4 constructs lacking either the calmodulin binding (CAMK4 NCB), or autoinhibitory domains (CAMK4 NAI). We see that CAMK4 NAI has a 67% (n=5, p<.0001, t-Test) decrease in binding to C12ORF57-FLAG when compared to WT CAMK4. CAMK4 NCB shows no change in binding to C12ORF57 suggesting that the autoinhibitory domain is essential to the C12ORF57 interaction with CAMK4(n=8, p=.2935) (**Figure 3.6 C**). To test whether mutations in human patients could also disrupt the CAMK4/C12ORF57 interaction, we performed immunoprecipitation on both wildtype and L51Q mutant C12ORF57. Under these conditions we found that the L51Q mutation decreased the co-immunoprecipitation for CAMK4 by 39% (N=8, p<.0001) compared to wildtype C12ORF57 protein (**Figure 3.6D**). Our initial yeast-two-hybrid and co-immunoprecipitation experiments indicated that C12ORF57 bound to CAMK4 in a domain found between residues 300-600. CAMK4 has known roles in neuronal outgrowth, as well as homeostasis of neuronal excitation (Redmond *et al* 2002). Therefore, the interaction between C12ORF57 and CAMK4 may be a promising candidate to explain the changes in neuronal outgrowth and excitability seen in *Grcc10-/-* neurons. We therefore sought to determine the effects of C12ORF57 on activation of CAMK4.

To directly analyze the changes in the activation and function of CAMK4 in the absence of C12ORF57, we utilized the CRISPR/Cas9 system to mutagenize *C12ORF57* in HEK293 cells. Because our data suggests that C12ORF57 binds to the autoinhibitory domain of CAMK4, we sought to determine whether CAMK4 phosphorylation and localization was affected by loss of C12ORF57. Subcellular fractionation in *Grcc10 -/-* mouse brains show a 34% decrease in total CAMK4 and a 52% decrease in pThr200 CAMK4 when compared to *Grcc10-/-* brains(**Figure 3.7 A**). The cytoplasmic fraction in turn shows a significant increase (19%) in CAMK4 in *Grcc10-*

/- compared to WT Brains, suggesting a shift in CAMK4 from nuclear (active) to cytoplasmic (inactive) in *Grcc10 -/-* cells . To further determine the effect of C12ORF57 on CAMK4 activity we performed an *in vitro* CAMK4 kinase activity assay. *In vitro* CAMK4 kinase assays show that while the addition of C12ORF57 to CAMK4 does not significantly change the activity of the kinase (**Figure 3.7C**). Previous work has shown PPP1CA, the catalytic subunit of PP1 can inactivate CAMK4 *in vitro* and *in vivo* by binding to residues 306-323*,* which we have shown above is the site for C12ORF57 binding. We therefore hypothesized that the binding of C12ORF57 to CAMK4 at amino acids 306-323 could lead to the dissociation of PPP1CA from CAMK4 and decrease the rate by which PP1 dephosphorylates CAMK4. We utilized the same CAMK4 activity assay as before but incubated active phosphorylated CAMK4 with an equimolar amounts of PPP1CA, as well as with a mixture of PP1CA and C12ORF57. We found that incubating CAMK4 in PPP1CA reduces its kinase activity by approximately 50%. When C12ORF57 is added and incubated with CAMK4 and PPP1CA we see no decrease, while the addition the L51Q mutant had no protective effect (**Figure 3.7C**) These data suggests that C12ORF57 promotes CAMK4 phosphorylation by blocking the activity of PP1.

Loss of C12ORF57 decreases CREB and signaling downstream of CAMK4

Having shown that C12ORF57 binds CAMK4 and increases its activity we sought to determine the effect on downstream effectors of CAMK4. Previous work has shown that the primary effector of CAMK4 is cAMP response element-binding protein 1(CREB1), which is phosphorylated at its Ser 133 residue (Mayr *et al* 2001, Gonzalez *et al* 1991 Gonzalez *et al* 1989). Phosphorylation at Ser133 is necessary for CREB activity, and while the majority of CREB is nuclear, in neurons, phosphorylation seems to drive localization of dendritic localized protein, suggesting an extra-nuclear pool of CREB which responds rapidly and dynamically to neuronal activation(Crino *et al*, 1998). We therefore sought to determine changes in Ser133 phosphorylation in CREB in both our HEK293 cell lines and P0 mouse brains via western

blotting. Through this method we see a marked decrease in CREB phosphorylation at Ser133 in *Grcc10-/-* mouse brains by 33% (**Figure 3.7D**). *In vitro* immune histochemistry stains hippocampal neuronal culture shows a similar decrease 32% in pCREB in *Grcc10-/-* neurons compared to WT neurons on immunohistochemistry(**Figure 3.7 G).** To determine effects on transcriptional activity of CREB we performed dual luciferase assays on our HEK293 17T cells with a CRE element in control of a firefly luciferase. We see a 25% decrease in luminescence in *Grcc10 -/-* cells when compared to wild type cells without a change in overall transcription. Transfection with C12ORF57 restored CREB signaling (Figure 3.7E). We also see a decrease in CREB regulated downstream effectors, Arc/Arg3.1 by 49% (n=9, p=.0043, t-test) respectively on western blotting in P0 mouse cortex (**Figure 3.7F**) We also see a decrease in Arc in *Grcc10-/- in vitro* hippocampal neurons by 64%. All this suggests that CREB signaling is reduced with the loss of C12ORF57 may be responsible for the phenotypes seen in both mice and humans and brains.

Loss of *Grcc10/C12ORF57* results in a decrease in cortical neuronal neurite outgrowth

We have established that C12ORF57 is expressed in cortical neurons throughout all points of cortical development, we sought to determine what effects loss of Grcc10 neuronal growth and development. We then sought to determine if there were changes in neuronal morphology. Previous data has shown that loss of CAMK4 and CREB signaling diminishes both neurite complexity and length. As we have demonstrated that C12ORF57 seems to have a positive regulatory effect on CAMK4 signaling pathways we sought to determine if loss of C12ORF57 had a similar effect on dendritic maturation and length. Culture of primary cortical pyramidal neurons cultured P0 mice showed a severe decrease in the dendritic complexity as quantified by Sholl analysis of *Grcc10 -/-* neurons when compared to *Grcc10 +/-* and *Grcc10 +/+* neurons. (**Figure 3.8A**). We also performed Sholl analysis on *in situ* Golgi stained pyramidal cortical neurons in postnatal day 0, 7, and 21 and we found a consistent decrease in neuronal

arborization *Grcc10 -/-* mice compared to WT mice (p=.541 n=3, p>.001, n=3, p>.001 n=3) (**Figure 3.8B**). This data suggests that the loss of *Grcc10* leads to a failure or neuronal maturation and development of secondary, tertiary and tertiary neurites as the neuron develops. This neuronal outgrowth phenotype is similar to previous genes associated with agenesis of the corpus callosum such as Cited2(Fame *et al* 2016)(Togawa *et al* 2012). This suggests that C12ORF57 has a crucial role in neurite outgrowth phenotype, specifically in the secondary and tertiary branching and neurite maturation, while not seeming to effect overall neuronal proliferation, which is consistent with our observation in both human patients who do not display microcephaly or other proliferation or migration defects such as polymicrogyria.

We also sought to determine whether C12ORF57's positive regulation of CAMK4 signaling could be responsible for this neuronal outgrowth phenotype. To this end we performed a series of rescue experiments in primary cortical neurons in which we transfected both CAMK4 and CREB into the primary neuronal culture. We see that transfection of CAMK4 and a constitutively active CAMK4 into primary cortical pyramidal neurons restores the neurite arborization, while CAMK4 a dominant negative mutation (Thr200Ala) fails to rescue the neurite arborization phenotype in *Grcc10-/-* neurons. (**Figure 3.8B**).

Discussion

Grcc10-/- mouse is a useful tool for studying the role of Temtamy syndrome in humans

Appreciation of C12ORF57's role in human disease has increased with the discovery new patient cases and the recognition of its importance in normal brain development. Early estimates place 1.5% of intellectual disability in Arab American populations with a primary genetic cause. In this study we have described the first mammalian model of homozygous loss of function C12ORF57. We see that C12ORF57 mutant mice share both the shortened corpus callosum phenotype as well as a seizure phenotype analogous to the corpus callosum and

epilepsy findings in human Temtamy patients. This animal model is the first described animal model for Temtamy syndrome and will provide a useful tool for further elucidation of the biochemical function of Grcc10/C12ORF57. Postnatal mortality remains a issue for this model which would be addressed through our development of conditional organ specific mouse knockout models for *Grcc10 -/-.*

C12ORF57/Grcc10 modulates CAMK4 and CREB signaling

Furthermore, this study has provided a plausible biochemical mechanism through positive modulation of CAMK4 and CREB signaling. We have shown that the interaction between Camkinin and CAMK4 is modulated by the autoinhibitory domain of CAMK4 which binds protein phosphatases PP1 and PP2 and that the loss of *Grcc10* decreases the amount of nuclear CAMK4. Furthermore we show that C12ORF57 is able to abrogate the negative effect of the catalytic unit of PPP1CA on CAMK4 *in vitro* (**Figure 3.7**) and that a downstream targets of CAMK4, CREB, has reduced phosphorylation. We therefore hypothesize the on possible mechanism of Camkinin activity in neurons is through binding to CAMK4 at its autoregulatory domain and preventing it from dephosphorylation by PP1 and therefore increasing the phosphorylation of downstream targets such as CREB(**Figure 3.8**). Previous work has established that neurotransmitters can induced calcium waves across the immature and developing brain play a crucial role in neuronal development (Mayer *et al* 2019), Garaschuk *et al* 2000) C12ORF57's effect on sensitivity calcium signaling through CAMK4 may position it as an important regulator of the sensitivity of various cells and brain regions to these waves of activity, providing a crucial fine tuning in brain development.

C12ORF57 plays a novel and crucial role in electrical homeostasis and Seizure pathology

Epilepsy are a common feature and source of morbidity among C12ORF57 patients. Furthermore, the majority of these patient's epilepsy is medically intractable, and the exact etiology of the seizures themselves are unknown. Our data suggests that C12ORF57 acts as a crucial tuning mechanism for neuronal excitability. We show that *Grcc10-/-* mice are more

susceptible to kainic acid seizures and we observed spontaneous seizures in *Grcc10-/-* mice (**Figure 3.2**). We see that *Grcc10* has activity dependent activity, and *Grcc10-/-* hippocampal neurons fail to aborize compared to their wild-type counterparts. Loss of *Grcc10-/-* in mouse hippocampal neurons results in a large increase in both the number of GluA2 positive synapses and increase in mEPSC suggesting an increase in overall neuronal excitability(**Figure 3.4**)**.**

A Proposed Model for C12ORF57/Camkinin activity

Given our data we propose the C12ORF57/Camkinin functions by binding to CAMK4 auto inhibitory domain and preventing its dephosphorylation by protein phopshpatases. This increases the activity of CAMK4 and thereby increases phosphorylation of downstream activators such as CREB and which increase expression of Arc. Arc then increases endocytosis of surface GluA2 receptors, reducing overall neuronal excitability. The loss of Camkinin results in a reduction in CAMK4 activity and Arc expression and in increases in GluA2 surface expression which in turn leads to a higher level of overall neuronal excitability and an increase in sensitivity to proconvulsant in mouse knockout models. This model provides a plausible explanation behind the epilepsy seen in human patients as well as providing a potential targetable pathway to treat seizures in these patients.

A

```
H.sapiens     -MASASTQPAALSAEQAKVVLAEVIQAFSAPENAVRMDEARDNACNDMGKMLQFVLPVATQIQQ  63
M.musculus    -MASASAQPAALSAEQAKVVLAEVIQAFSAPENAVRMDEARDNACNDMGKMLQFVLPVATQIQQ  63
G.gallus      MAASAQAPPPALSAEQAKVVLAEVIKAFGAPENVQRMDEARENACNDMGKMLQFLLPVATQIQQ  64
D.rerio       -MASAPAQQPTLTVEQARVVLSEVIQAFSVPENAARMEEARESACNDMGKMLQLVLPVATQIQQ  63

H.sapiens     EVIKAYGFSCDGEGVLKFARLVKSYEAQDPEIASLSGKLKALFLPPMTLPPHGPAAGGSVAAS  126
M.musculus    EVIKAYGFSCDGEGVLKFARLVKSYEAQDPEIASLSGKLKALFLPPMTLPPHGPASGSSVAAS  126
G.gallus      DVIKAYGFSSDGEGVLKFARLIKSYESQDPEIASMSGKLKALFLPPMTLPPHG-AGIGGVAAS  126
D.rerio       EVIKAYGFNNEGEGVLKFARLVKMYETQDPEIAAMSVKLKSLLLPPLSTPPIGSGIPTS----  122
```

B

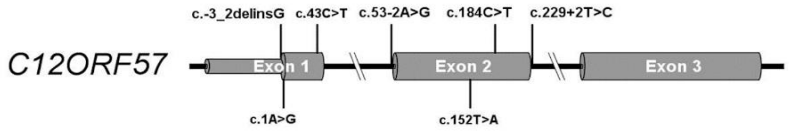

Figure 3.1 C12ORF57 is highly conserved and LoF mutations are causative in Temtamy syndrome A) Comparison of amino acid sequence between human (C12ORF57) and mouse

(GRCC10), and zebrafish (Grcc10) homologues shows a high level of amino acid identity of between sequences (98% in Mus *musculus*, 88% in G. gallus and 72% *Danio* rerio)B) Mutations reported in 54 human patients in C12ORF57 currently in the literature. Missense mutations are listed blow the gene. and nonsense, splice site, and frame shift mutations listed above. This figure has been adapted from a previous figure in (Alrakaf L 2018)

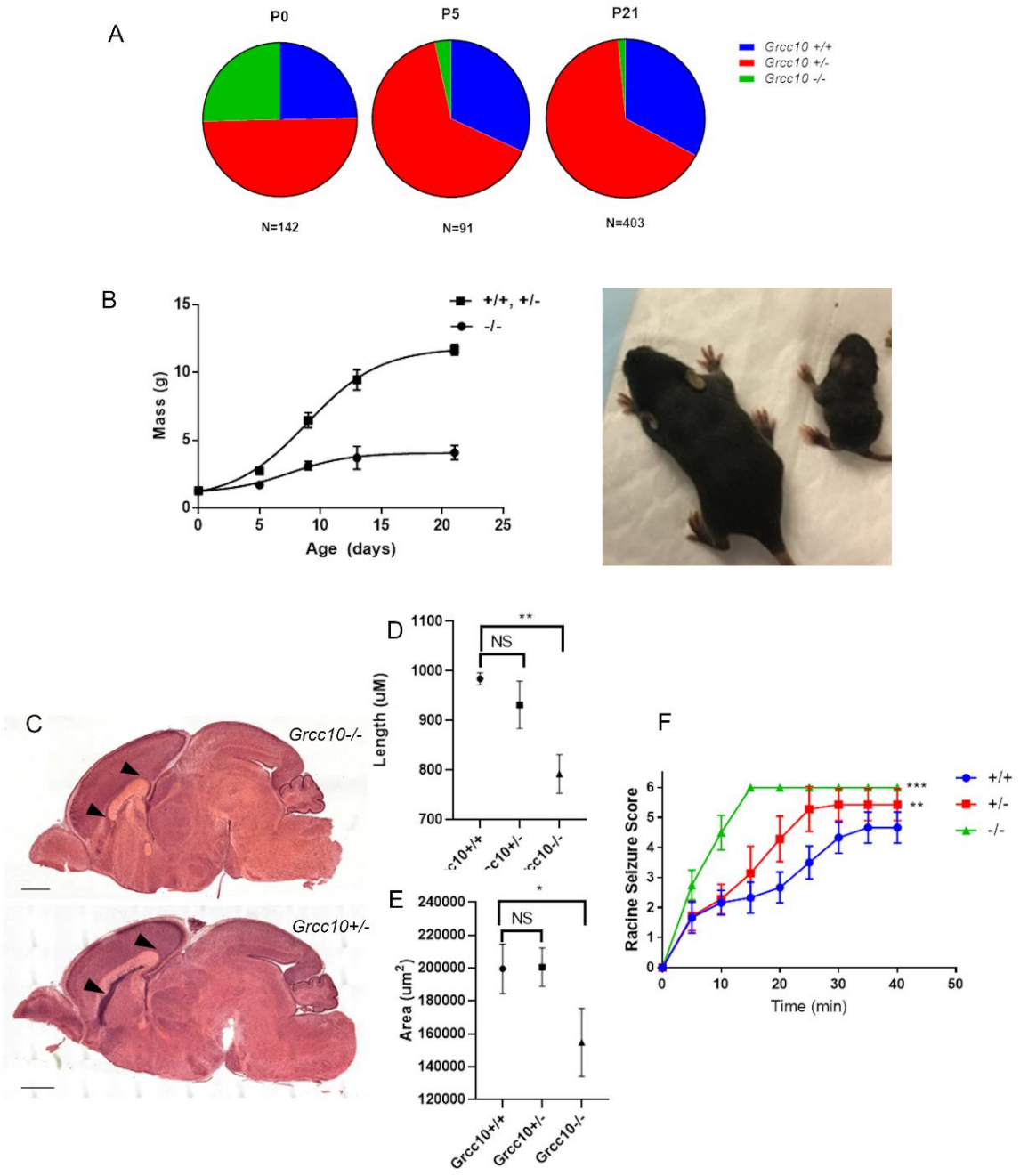

Figure 3.2 *Grcc10 -/-* mice recapitulate several important phenotypes of the human disease. A) At P0, *Grcc10 +/- x Grcc10 +/-* litters have expected 1:2:1 Mendelian ratios (p=.871, Chi Squared test). The majority of *Grcc10-/-* pups die by P2, with <5% surviving after P5 (p<.00001, Chi Squared). B) *Grcc10-/-* mice show a progressive loss of body mass from birth compared to wildtype and heterozygous littermates (75%, P<.0001, T, test) by P21as seen in P16 WT (left) and KO mice (right) littermates. C) *P0 Grcc10 -/-* mouse brain (top, black arrows) show a

shortened dysmorphic corpus callosum when compared to WT (bottom, black arrows) with a D)26% and decrease in average length and E) 20% cross sectional area at the midline (p=.0182, p=.0017, Mann Whitney). Scale Bar 500 um **F)** *Grcc10 -/-* mice (N=5) progress to higher Racine Seizure stages than +/+ (n=7) and +/- (n=7) mice as well as reaching a higher overall average racine stage after 60 minutes post dosing with 20 ug/mg.

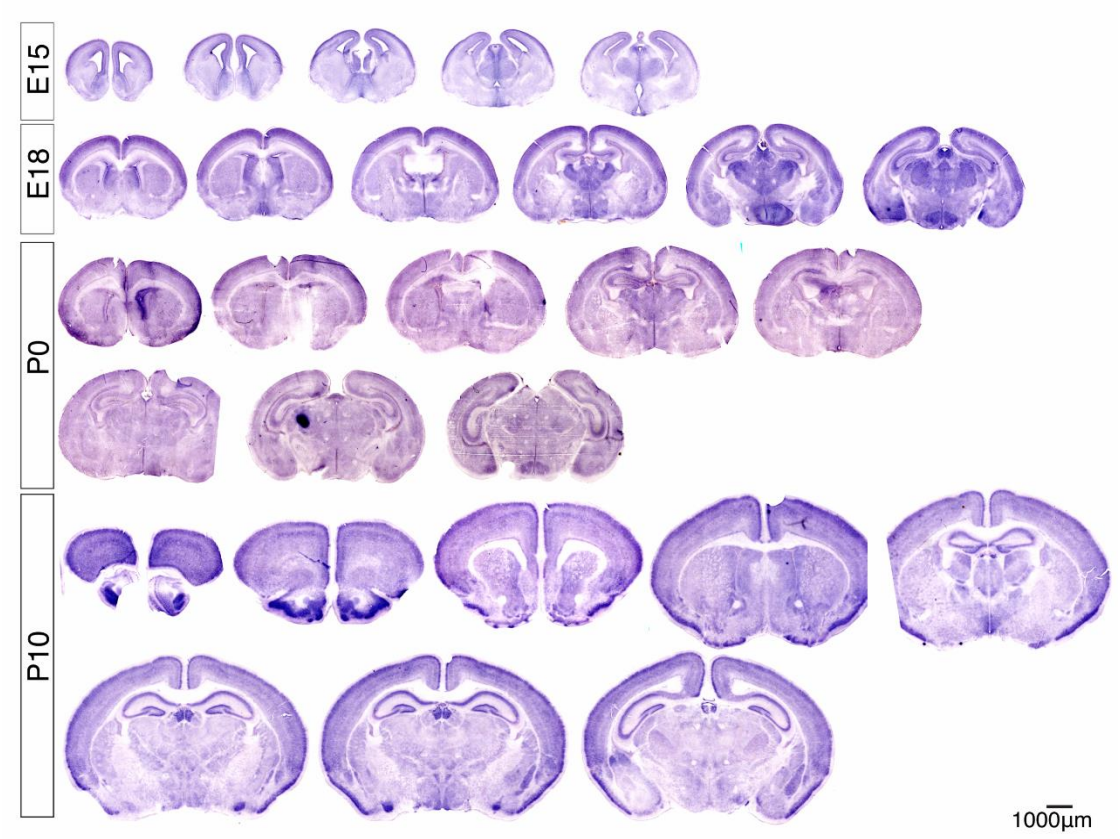

Figure 3.3: Grcc10 is expressed throughout the developing mouse brain *Grcc10* expression was detected at ventricular zone, glial wedge, and cortical plate at E15. In addition to the regions as seen at E15, the expression of *Grcc10* was observed at hippocampus, cingulate cortex, and indusium griseum at E18. The expression of *Grcc10* persisted at those regions for P0 and P10.we see the highest level of expression in the early postnatal and late embryonic period.

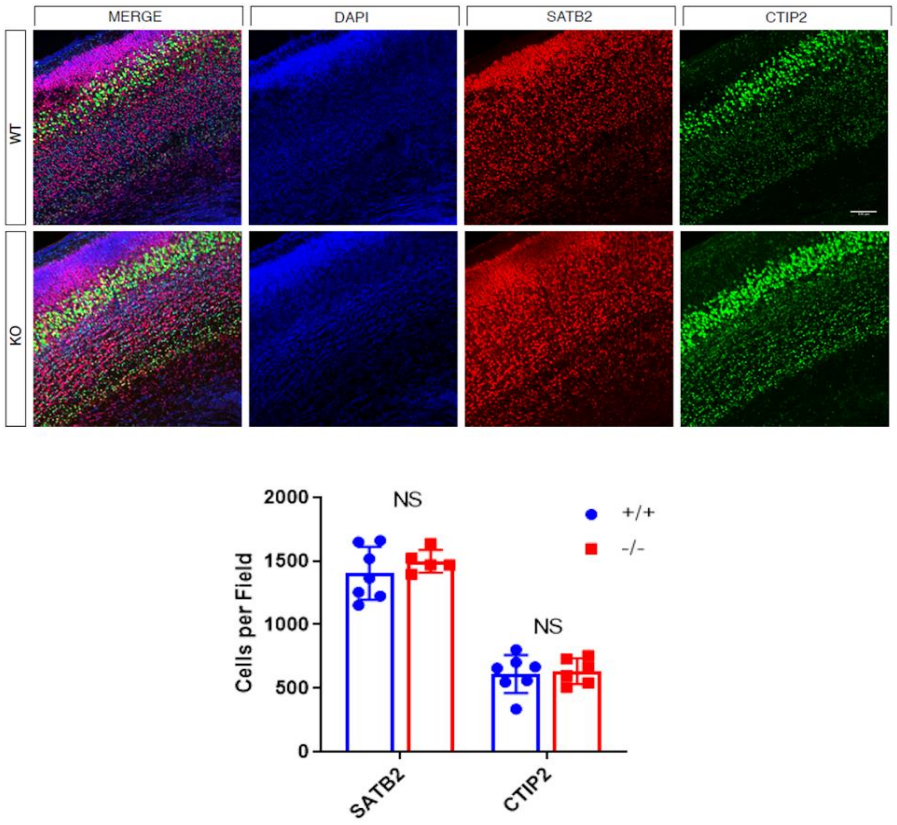

Figure 3.4 Loss of Grcc10 causes no change in overall cortical neuronal numbers

P0 mouse cortex was stained with dAPI (blue) and for SATB2 (red) to label upper layer neurons and CTIP2 (green) lower layer neurons. We saw no significant change in either SATB2 or CTIP2 neurons between wild type or Grcc10 KO (lower) mouse brains. (p=.652, p=.588)

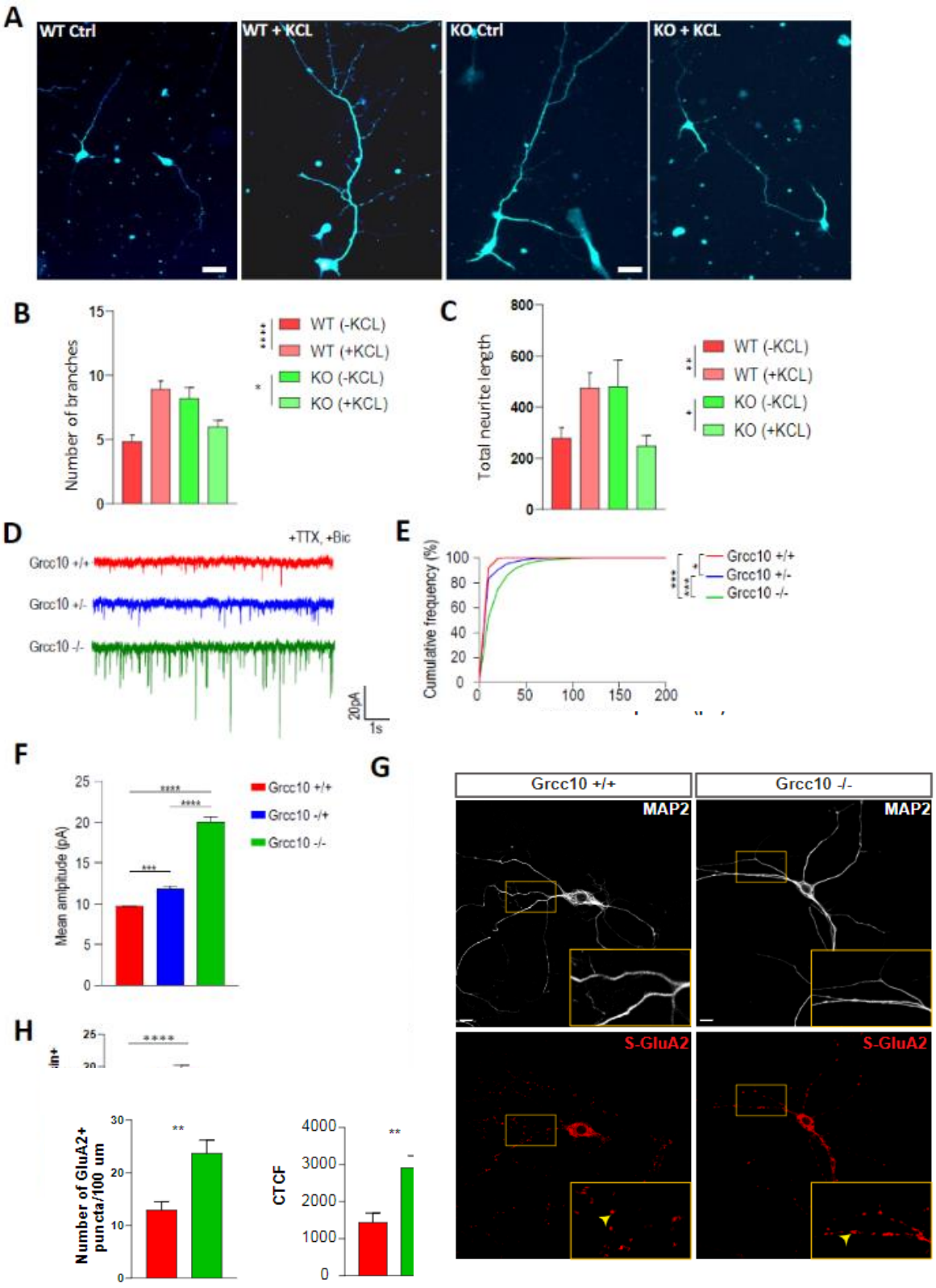

Figure 3.5: C12ORF57/Camkinin has an activity dependent effect in neurons
A, Representative pictures of 7 days in vitro WT and KO neurons transfected with a GFP expressing lentivirus for morphological tracing and treated or not with high concentration of

KCL. Scale bar (25 um). B, Quantification of the total number of branches and C, total neurites length before and after KCL treatment. (Student t-test, p*=0.0356, p**=0.0088, p***<0.0001). D, representative raw recordings of whole-cell mEPSCs from 15 div hippocampal neurons (top) Grcc10 -/+, (bottom) Grcc10 -/-. E, Cumulative histogram of mEPSCs amplitude in pA (p<0.0005, Kruskal-Wallis test). F, Mean mEPSCs amplitude (p<0.0001, Student t-test). G, Representative pictures of 20 days in vitro WT and KO neurons immuno-stained for GluA2 Smaller bottom panels are zoom-ins of yellow dashed boxes. Scale bar (50 um). F, Quantification of the mean number of GluA2 positive puncta per 50 um of neurites of WT and KO neurons (Student t-test, p****<0.0001). G, Representative image of GluA2 staining.

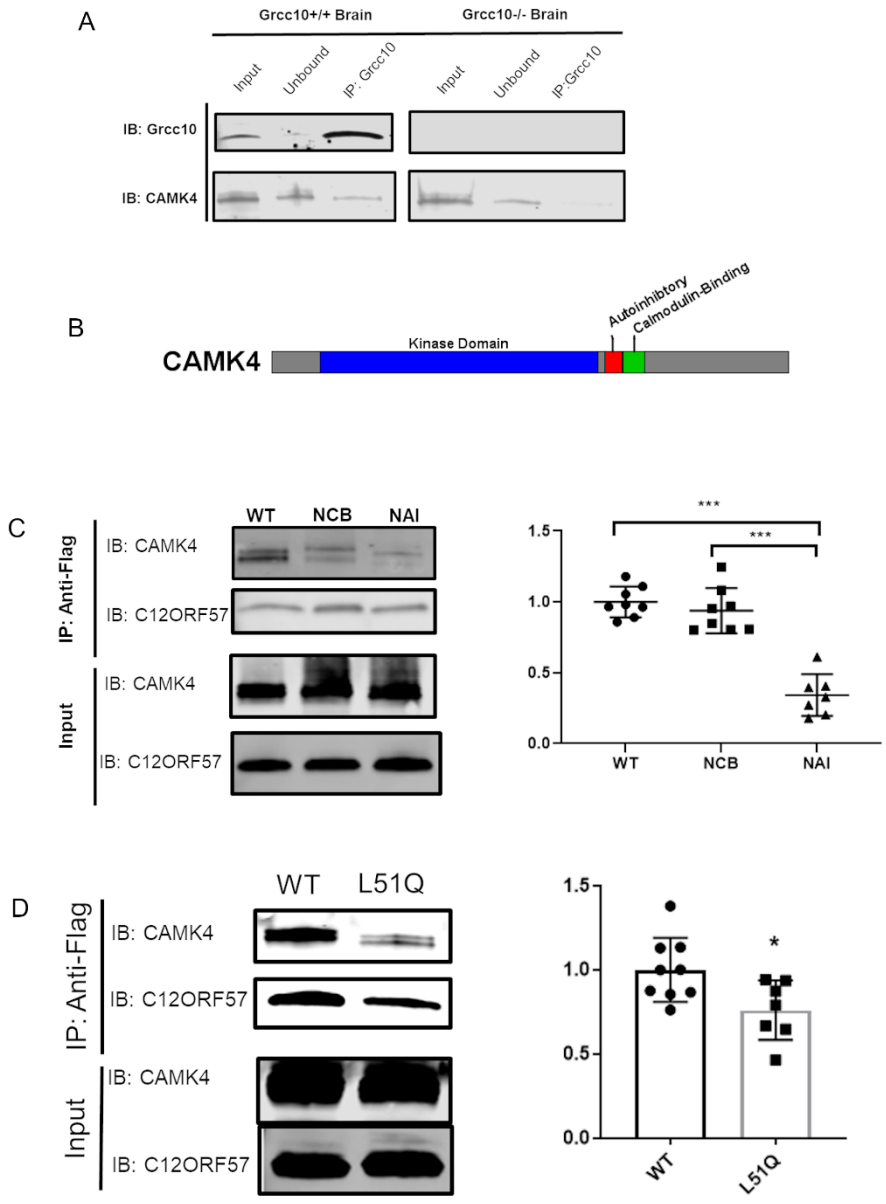

Figure 3.6 C12ORF57/GRCC10 binds to Calcium/Calmodulin Associated Kinase 4 Autoregulatory Domain A) CAMK4 (bottom) coimmunoprecipitates with Grcc10 with anti-GRCC10 antibody (top) in WT whole mouse brain lysates (left) but not in *Grcc10-/-* Brain (right)) B) CAMK4 with three major regions recognized The large kinase domain (blue) (AA: 46-300), followed by a autoregulatory domain (red) (AA305-321) and calmodulin binding domain (green) (AA 322-341) C) Deletion of the autoregulatory domain (AA 305-321) (NR) reduces the co-

immunoprecipitation efficiency with C12ORF57-FLAG drops by 63% (p=.0005, T-test) when compared to wild type CAMK4. Deletion of the calmodulin binding domain (NC) results in no significant change in coimmunoprecipitation of C12ORF57when compared to WT CAMK4 (p=.82174, T, test) suggesting the necessity of the autoregulatory domain for regular C12ORF57/CAMK4 interaction D) C12ORF57 c.t152a/L51Q, mutation found in human patients reduces CAMK4 co immunoprecipitation by 24% (p=.0218, T. test) when compared to wildtype C12ORF57 in HEK29317T lysates

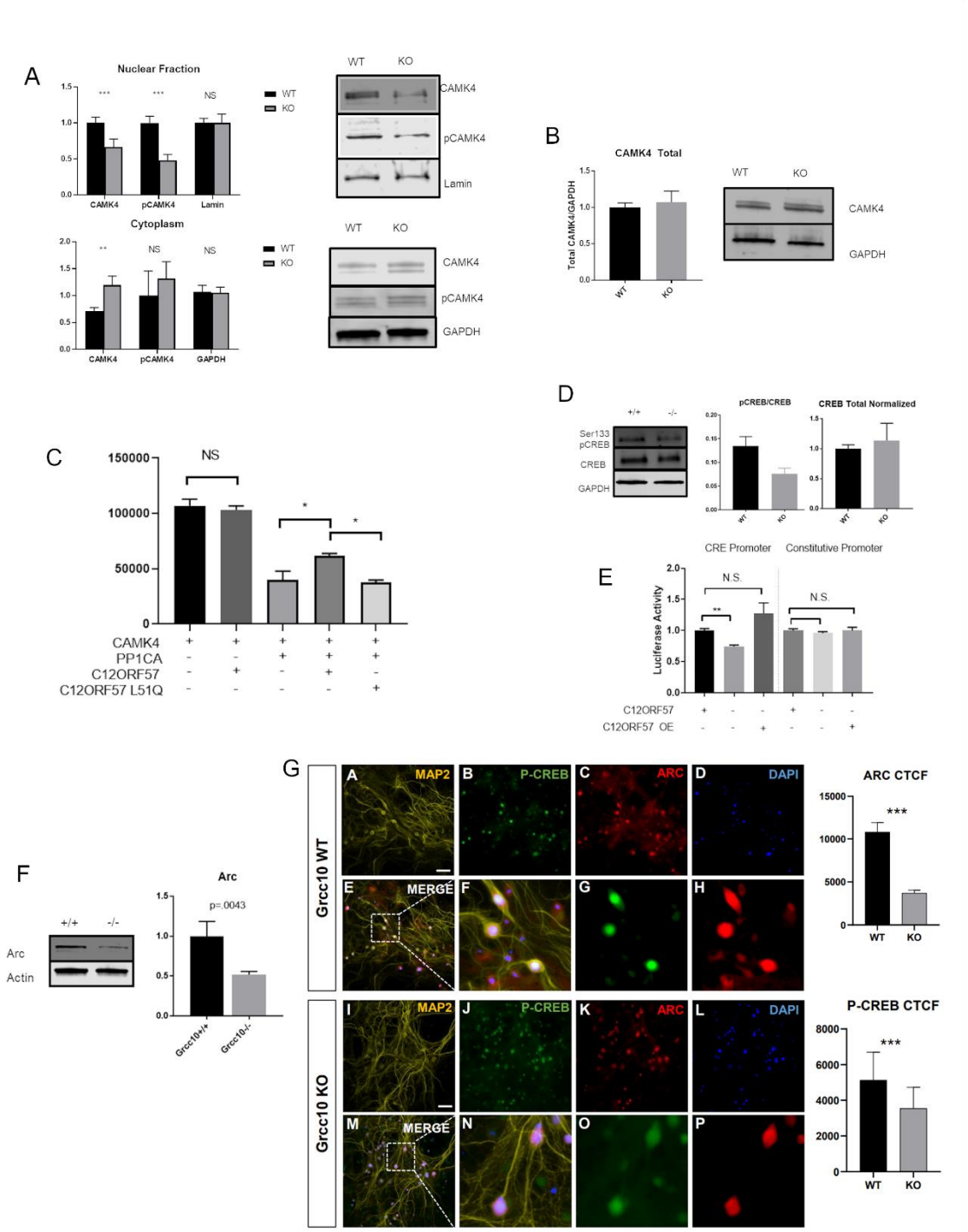

Figure 3.7 Loss of C12OR57 Reduces CAMK Phosphorylation and Downstream signaling **A)** Western blot quantification of Subcellular fractionation on mouse brains shows a 43% (p=.00018, T.test) decrease in nuclear CAMK4, with a similar 44% decrease in pThr200 CAMK4 in *Grcc10-/-* mice when compared to wild type. There is a 36% increase in CAMK4 in the

cytoplasmic fraction in *Grcc10-/-* brains, suggesting a shift of CAMK4 from nuclear to cytoplasmic with the loss of *Grcc10.* **B)** Overall levels of CAMK4 in whole cell fractions remains the same(p=.833, T. test). C) *In vitro* CAMK4 kinase activity assays show no change in CAMK4 activity with the addition of C12ORF57 alone, however with the addition of Protein phosphatase Catalytic unit 1 (PP1CA), kinase activity of CAMK4 decreases and C12ORF57 addition provides a protective effect. Addition of mutant C12ORF57 p.L51Q has no protective effect. D) CREB phosphorylation at residue Ser133, is reduced by 53% in *Grcc10-/-* mouse brains when compared to wild type brains, while overall CREB levels remain constant. **C)** Dual luciferase assays in HEK293 17T cells show a 25.4% (p=.0012) decrease in CREB activity in C12ORF57-/- cells when compared to wild type cells. No changes seen in the control constitutive promoter. **D)** P0 mouse cortex lysate shows a decrease in downstream CREB targets Arc (53%, p=.0043 and 52% p=.0036) respectively on western blot. **E)** Immunohistochemistry of hippocampal neurons and quantification of corrected total cell fluorescence shows a statistically significant decrease in Arc and pCREB levels in *Grcc10-/-* neurons compared to *Grcc10+/+* neurons. Representative pictures of 25 DIV Grcc10+/+ hippocampal neurons (upper panels) and Grcc10 -/- neurons (lower panels) stained for MAP2 (yellow), Phospho-CREB (green), ARC (red) and DAPI (blue). E, M (merge). F, G and H (zoom out of dotted square of merge and single channels).

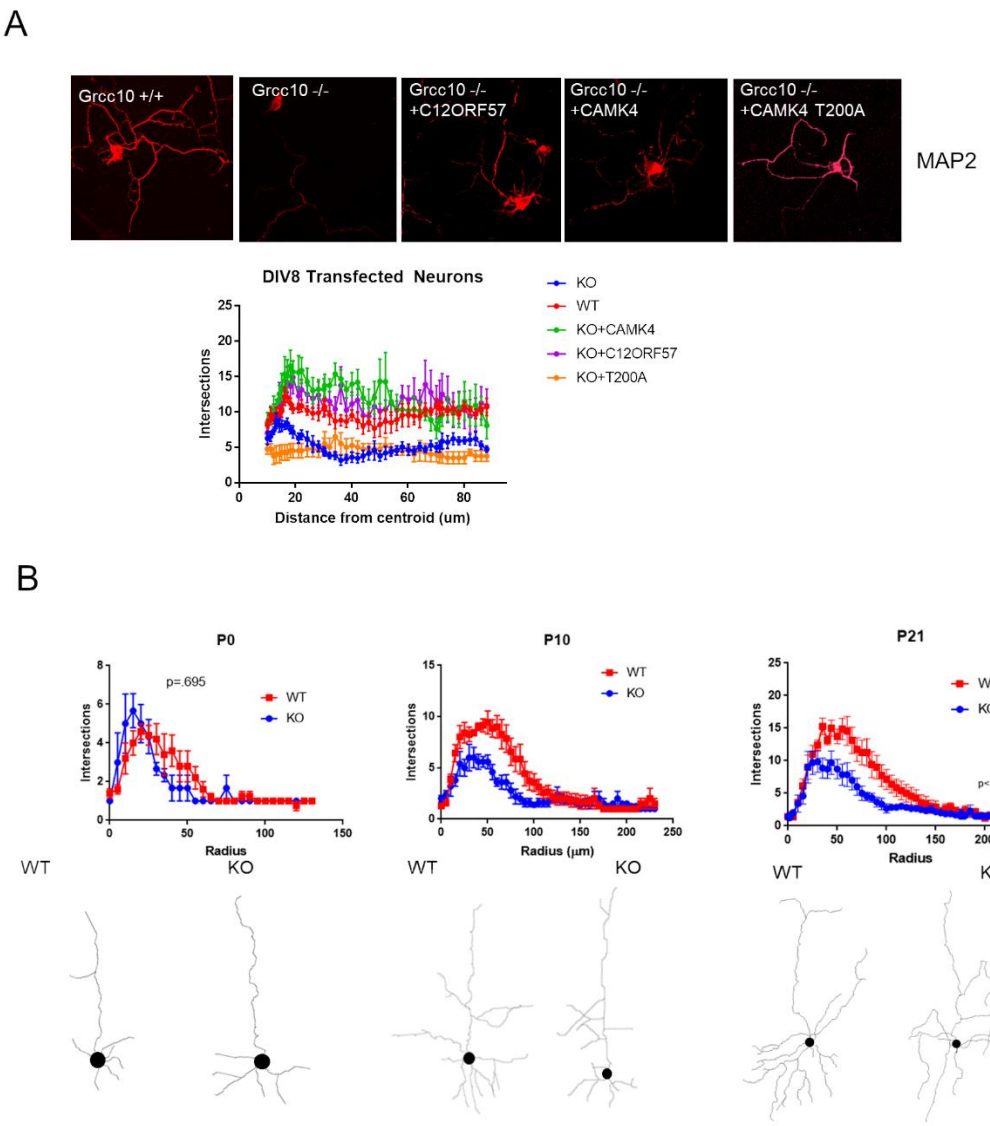

Figure 3.8 Loss of Grcc10 reduces dendritic complexity in cortical neurons

A) *In vitro* cultured cortical neurons a DIV8 show a decrease in overall complexity of neurites in *Grcc10 -/-* neurons (blue) when compared to WT (red) when measured by Sholl analysis. Transfection of C12ORF57 (Purple) and CAMK4 (Green) into *Grcc10 -/-* neurons rescues this phenotype and restores dendritic arborization. Transfection of a phosphodead CAMK4 (T200A) does not restore normal neuronal aborization. Representative pictures shown above. B) Golgi staining of *in situ* cortical neurons in mice also shows no difference in dendritic complexity in cortical neurons in wild-type vs knockout neurons at P0 but shows a loss of complexity in neurons in P10 and P21 mice. Representative traces shown below.

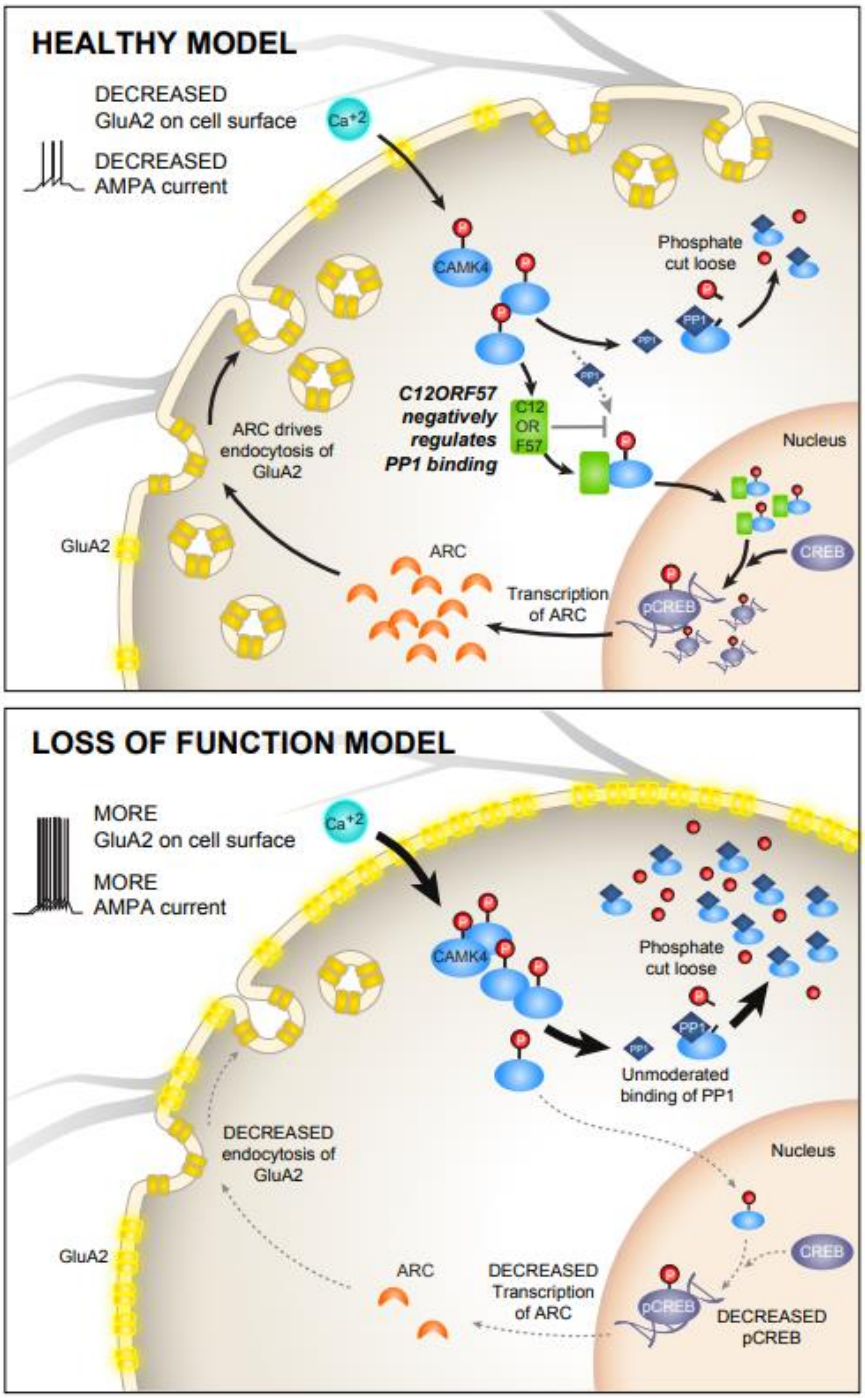

Figure 3.9 Proposed model for C12ORF57/Camkinin function Given our data we propose the C12ORF57/Camkinin function(top). An increase in neuronal activity (represented by the flux of

calcium ions) increases CAMK4 phosphorylation and C12ORF57/Camkinin binds to CAMK4 prevent its dephosphorylation by protein phophotases. This increases the activity of CAMK4 and thereby increases phosphorylation of downstream activators such as CREB and which increase expression of Arc. Arc then increases endocytosis of surface GluA2 receptors, reducing overall neuronal excitability. The loss of Camkinin results in a reduction in CAMK4 activity and Arc expression and in increases in GluA2 surface expression which in turn leads to a higher level of overall neuronal excitability and an increases in sensitivity to proconvulsants in mouse knockout models (Bottom).

Materials and Methods

Grcc10 Mouse Lines

(Cg)-*Grcc10*$^{tm1.1(KOMP)Vlcg}$ on a B6N/J background strain were obtained from Jackson lab. Mice were maintained at 12 hour light-dark cycle and food and water were maintained *ad libitum.* Mice were not randomized for experimentation.

Corpus Callosum Area analysis

Mice were sectioned at P0 days of age. Serial sections of 15 um thickness were taken and selected near the midline. A blinded observer was given the images and instructed to outline the corpus callosum in imageJ as well as measure consistently between the rostral and caudal ends of the corpus callosum and the cortex. Mean are and length of corpus callosum between genotypes were compared statistically using a Welch's T. Test.

Generation of CRISPR cell lines

CRISPR cell lines were generated from HEK293 17T using a pSpCAs9(BB)-2A- Puro (PX459) (Ran *et al* 2013) V2.0 plasmid backbone with the following sgRNA.

Human: GATAACGCCTGCAACGACAT

HEK29317T cells were transfected with using Lipofectamine3000 reagent and cells were selected using puromycin at 2 uM concentrations.

C12ORF57 Antibody generation

C12ORF57 epitope was generated using a full length antigen of human C12ORF57 conjugated to a GST (NCBI9606) produced in BL21(DE3) competent *E.Coli.* and purified against a

Glutathione agarose (GE Lifescience 17075601). Rabbit polyclonal antibody was producing using Thermo Fisher Custom Polyclonal Antibody production.

Synaptosome Isolation and staining

Synaptosomes were isolated from whole P0 mouse brain using Syn-Per Synaptic Protein Extraction Reagent (ThermoScientific, 87793) on ice. Brains were homogenized using a dounce homogenizer and then spun at 1200xg for 10 minutes at 4 degree to separate the nuclei and unlysed cells.

CREB Reporter Dual Luciferase Assay

Wildtype and *C12ORF57-/-* HEK293T were plated in a 96 well plate at 20,000 cells per well. A *Renilla* luciferase under the control of a CRE promoter as well as a control firefly luciferase gene under a low level constitutive promoter (BPSBioscience, 60611) were transfected into both cell lines using Lipofectamine 3000. Cells were lysed and the luciferase activity was measured using a Dual luciferase kit (Thermofisher Scientific, 16186) on a Tecan Spark. Rescue experiments were performed by co-transtransfection of C12ORF57-myc-FLAG in a PCMV6-Sport vector utilizing lipofectamine 3000.

RT PCR C12ORF57

RNA was extracted from a pooled available human dermal fibroblast line and human patient fibroblasts Quik-RNA Microprep (Zymo R1055), and cDNA was produced using SuperScript IV VILO system (ThermoFisher Scientific, 11756500). Reverse transcriptase reaction was performed using the following primers:

C12ORF57/Camkinin

Forward: 5’-TGAGCGCTGAGCAAGC-3’

Reverse: CAGCTGAAGCCATAGGCTT

GAPDH

Forward: CATGTTCGTCATGGGGTGAAACA

Reverse: AGTGATGGCATGGACTGTGGTCAT

PCR Run cycle was run 95ºC melt 1 minute, then 30 cycles of 95ºC melt (30 sec) 55ºC anneal (30 seconds) 72^0C extension, followed by a final 7 minute extension. Bands were visualized on a 1% agarose gel using EtBR.

CAMK4 in vitro Assay

CAMK4 *in vitro* assay was performed using CAMK4 Kinase Enzyme System (Promega, V2915). Purified PPP1CA was obtained (Origene, TP7260246) and added a 50 uM concentration (1:2 molar ratio to CAMK4) and C12ORF57-Myc-FLAG was overexpressed in HEK293 Cells and purified via co-IP on ANTI-FLAG M2 Affinity gel (Millipore Sigma, A2220) with purification confirmed via western blot and added in an equimolar concentration to the reaction. All reactions were incubated for 15 minutes before the reaction was quenched. Luminesence was measured on a Tecan Spark with an integration time of 0.5 second per well.

Kainic Acid Sensitivity Test

Mice were weighed and dosed with 20 mg/kg of kanic acid injected intraperitoneally. Mice were then observed blinded to genotype and time at which each mouse entered or left each Racine stages was noted up to 1 hour. Racine stages are were used as described in Racine *et al* 1963.

Subcellular Fractionation

Tissue was homogenized in a Dounce homogenizer in fractionation buffer (20 mM HEPES pH7.4, 10 mM KCl, 2 mM $MgCl_2$, 1 mM EDTA, 1 mM EGTA, 0.2 mM DTT). Sample was passed through a 27 gauge needle 10 times and then centrifuged at 720xg for 5 minutes. Supernatant was removed and saved (Mixed cytoplasmic fraction). The remaining nuclear pellet was resuspended in 500 ul of fractionation buffer, and then centrifuged at 720xg for 10 minutes and the nuclei were lysed using .1%SDS. Mixed cytoplasmic fraction was centrifuged at 10,000 xg. To create the cytoplasmic fraction.

References

Akizu, N., N. M. Shembesh, T. Ben-Omran, L. Bastaki, A. Al-Tawari, M. S. Zaki, R. Koul, E. Spencer, R. O. Rosti, E. Scott, E. Nickerson, S. Gabriel, G. da Gente, J. Li, M. A. Deardorff, L. K. Conlin, M. A. Horton, E. H. Zackai, E. H. Sherr and J. G. Gleeson (2013). "Whole-exome sequencing identifies mutated c12orf57 in recessive corpus callosum hypoplasia." Am J Hum Genet 92(3): 392-400.

Alcamo, E. A., L. Chirivella, M. Dautzenberg, G. Dobreva, I. Farinas, R. Grosschedl and S. K. McConnell (2008). "Satb2 regulates callosal projection neuron identity in the developing cerebral cortex." Neuron 57(3): 364-377.

Alcamo, E. A., L. Chirivella, M. Dautzenberg, G. Dobreva, I. Farinas, R. Grosschedl and S. K. McConnell (2008). "Satb2 regulates callosal projection neuron identity in the developing cerebral cortex." Neuron 57(3): 364-377.

Alrakaf, L., M. A. Al-Owain, M. Busehail, M. A. Alotaibi, D. Monies, H. M. Aldhalaan, A. Alhashem, Z. N. Al-Hassnan, Z. A. Rahbeeni, F. A. Murshedi, N. A. Ani, A. Al-Maawali, N. A. Ibrahim, F. M. Abdulwahab, M. Alsagob, M. O. Hashem, W. Ramadan, M. Abouelhoda, B. F. Meyer, N. Kaya, S. Maddirevula and F. S. Alkuraya (2018). "Further delineation of Temtamy syndrome of corpus callosum and ocular abnormalities." Am J Med Genet A 176(3): 715-721.

Bartholdi, D., J. H. Roelfsema, F. Papadia, M. H. Breuning, D. Niedrist, R. C. Hennekam, A. Schinzel and D. J. Peters (2007). "Genetic heterogeneity in Rubinstein-Taybi syndrome: delineation of the phenotype of the first patients carrying mutations in EP300." J Med Genet 44(5): 327-333.

Bartsch, O., S. Schmidt, M. Richter, S. Morlot, E. Seemanova, G. Wiebe and S. Rasi (2005). "DNA sequencing of CREBBP demonstrates mutations in 56% of patients with Rubinstein-Taybi syndrome (RSTS) and in another patient with incomplete RSTS." Hum Genet 117(5): 485-493.

Bedeschi, M. F., M. C. Bonaglia, R. Grasso, A. Pellegri, R. R. Garghentino, M. A. Battaglia, A. M. Panarisi, M. Di Rocco, U. Balottin, N. Bresolin, M. T. Bassi and R. Borgatti (2006). "Agenesis of the corpus callosum: clinical and genetic study in 63 young patients." Pediatr Neurol 34(3): 186-193.

Benadiba, C., D. Magnani, M. Niquille, L. Morle, D. Valloton, H. Nawabi, A. Ait-Lounis, B. Otsmane, W. Reith, T. Theil, J. P. Hornung, C. Lebrand and B. Durand (2012). "The ciliogenic transcription factor RFX3 regulates early midline distribution of guidepost neurons required for corpus callosum development." PLoS Genet 8(3): e1002606.

Bonneau, D., A. Toutain, A. Laquerriere, S. Marret, P. Saugier-Veber, M. A. Barthez, S. Radi, V. Biran-Mucignat, D. Rodriguez and A. Gelot (2002). "X-linked lissencephaly with absent corpus callosum and ambiguous genitalia (XLAG): clinical, magnetic resonance imaging, and neuropathological findings." Ann Neurol 51(3): 340-349.

Britanova, O., C. de Juan Romero, A. Cheung, K. Y. Kwan, M. Schwark, A. Gyorgy, T. Vogel, S. Akopov, M. Mitkovski, D. Agoston, N. Sestan, Z. Molnar and V. Tarabykin (2008). "Satb2 is a postmitotic determinant for upper-layer neuron specification in the neocortex." Neuron 57(3): 378-392.

Byrd, S. E., D. C. Harwood-Nash and C. R. Fitz (1978). "Absence of the corpus callosum: computed tomographic evaluation in infants and children." J Can Assoc Radiol 29(2): 108-112.

Carrel, L. and H. F. Willard (2005). "X-inactivation profile reveals extensive variability in X-linked gene expression in females." Nature 434(7031): 400-404.

Chatila, T., K. A. Anderson, N. Ho and A. R. Means (1996). "A unique phosphorylation-dependent mechanism for the activation of Ca2+/calmodulin-dependent protein kinase type IV/GR." J Biol Chem 271(35): 21542-21548.

Chen, C. Y., C. H. Chan, C. M. Chen, Y. S. Tsai, T. Y. Tsai, Y. H. Wu Lee and L. R. You (2016). "Targeted inactivation of murine Ddx3x: essential roles of Ddx3x in placentation and embryogenesis." Hum Mol Genet 25(14): 2905-2922.

Chen, H. H., H. I. Yu, M. H. Yang and W. Y. Tarn (2018). "DDX3 Activates CBC-eIF3-Mediated Translation of uORF-Containing Oncogenic mRNAs to Promote Metastasis in HNSCC." Cancer Res 78(16): 4512-4523.

Crino, P., K. Khodakhah, K. Becker, S. Ginsberg, S. Hemby and J. Eberwine (1998). "Presence and phosphorylation of transcription factors in developing dendrites." Proc Natl Acad Sci U S A 95(5): 2313-2318.

Deuel, T. A., J. S. Liu, J. C. Corbo, S. Y. Yoo, L. B. Rorke-Adams and C. A. Walsh (2006). "Genetic interactions between doublecortin and doublecortin-like kinase in neuronal migration and axon outgrowth." Neuron 49(1): 41-53.

Dikow, N., M. Granzow, L. M. Graul-Neumann, S. Karch, K. Hinderhofer, N. Paramasivam, L. J. Behl, L. Kaufmann, C. Fischer, C. Evers, M. Schlesner, R. Eils, G. Borck, C. Zweier, C. R. Bartram, J. C. Carey and U. Moog (2017). "DDX3X mutations in two girls with a phenotype overlapping Toriello-Carey syndrome." Am J Med Genet A 173(5): 1369-1373.

Ding, J. and E. Delpire (2014). "Deletion of KCC3 in parvalbumin neurons leads to locomotor deficit in a conditional mouse model of peripheral neuropathy associated with agenesis of the corpus callosum." Behav Brain Res 274: 128-136.

Dode, C., J. Levilliers, J. M. Dupont, A. De Paepe, N. Le Du, N. Soussi-Yanicostas, R. S. Coimbra, S. Delmaghani, S. Compain-Nouaille, F. Baverel, C. Pecheux, D. Le Tessier, C. Cruaud, M. Delpech, F. Speleman, S. Vermeulen, A. Amalfitano, Y. Bachelot, P. Bouchard, S. Cabrol, J. C. Carel, H. Delemarre-van de Waal, B. Goulet-Salmon, M. L. Kottler, O. Richard, F. Sanchez-Franco, R. Saura, J. Young, C. Petit and J. P. Hardelin (2003). "Loss-of-function mutations in FGFR1 cause autosomal dominant Kallmann syndrome." Nat Genet 33(4): 463-465.

Edwards, T. J., E. H. Sherr, A. J. Barkovich and L. J. Richards (2014). "Clinical, genetic and imaging findings identify new causes for corpus callosum development syndromes." Brain 137(Pt 6): 1579-1613.

Elvira, G., S. Wasiak, V. Blandford, X. K. Tong, A. Serrano, X. Fan, M. del Rayo Sanchez-Carbente, F. Servant, A. W. Bell, D. Boismenu, J. C. Lacaille, P. S. McPherson, L. DesGroseillers and W. S. Sossin (2006). "Characterization of an RNA granule from developing brain." Mol Cell Proteomics 5(4): 635-651.

Englund, C., A. Fink, C. Lau, D. Pham, R. A. Daza, A. Bulfone, T. Kowalczyk and R. F. Hevner (2005). "Pax6, Tbr2, and Tbr1 are expressed sequentially by radial glia, intermediate progenitor cells, and postmitotic neurons in developing neocortex." J Neurosci 25(1): 247-251.

Enslen, H., H. Tokumitsu, P. J. Stork, R. J. Davis and T. R. Soderling (1996). "Regulation of mitogen-activated protein kinases by a calcium/calmodulin-dependent protein kinase cascade." Proc Natl Acad Sci U S A 93(20): 10803-10808.

Esmaeeli Nieh, S., M. R. Madou, M. Sirajuddin, B. Fregeau, D. McKnight, K. Lexa, J. Strober, C. Spaeth, B. E. Hallinan, N. Smaoui, J. G. Pappas, T. A. Burrow, M. T. McDonald, M. Latibashvili, E. Leshinsky-Silver, D. Lev, L. Blumkin, R. D. Vale, A. J. Barkovich and E. H. Sherr (2015). "De

novo mutations in KIF1A cause progressive encephalopathy and brain atrophy." Ann Clin Transl Neurol 2(6): 623-635.

Esmaeeli Nieh, S., M. R. Madou, M. Sirajuddin, B. Fregeau, D. McKnight, K. Lexa, J. Strober, C. Spaeth, B. E. Hallinan, N. Smaoui, J. G. Pappas, T. A. Burrow, M. T. McDonald, M. Latibashvili, E. Leshinsky-Silver, D. Lev, L. Blumkin, R. D. Vale, A. J. Barkovich and E. H. Sherr (2015). "De novo mutations in KIF1A cause progressive encephalopathy and brain atrophy." Ann Clin Transl Neurol 2(6): 623-635.

Fame, R. M., J. L. MacDonald, S. L. Dunwoodie, E. Takahashi and J. D. Macklis (2016). "Cited2 Regulates Neocortical Layer II/III Generation and Somatosensory Callosal Projection Neuron Development and Connectivity." J Neurosci 36(24): 6403-6419.

Fierro, M., A. J. Martinez, J. W. Harbison and S. H. Hay (1977). "Smith-Lemli-Opitz syndrome: neuropathological and ophthalmological observations." Dev Med Child Neurol 19(1): 57-62.

Fitzky, B. U., M. Witsch-Baumgartner, M. Erdel, J. N. Lee, Y. K. Paik, H. Glossmann, G. Utermann and F. F. Moebius (1998). "Mutations in the Delta7-sterol reductase gene in patients with the Smith-Lemli-Opitz syndrome." Proc Natl Acad Sci U S A 95(14): 8181-8186.

Floor, S. N., K. J. Barkovich, K. J. Condon, K. M. Shokat and J. A. Doudna (2016). "Analog sensitive chemical inhibition of the DEAD-box protein DDX3." Protein Sci 25(3): 638-649.

Floor, S. N., K. J. Condon, D. Sharma, E. Jankowsky and J. A. Doudna (2016). "Autoinhibitory Interdomain Interactions and Subfamily-specific Extensions Redefine the Catalytic Core of the Human DEAD-box Protein DDX3." J Biol Chem 291(5): 2412-2421.

Fransen, E., V. Lemmon, G. Van Camp, L. Vits, P. Coucke and P. J. Willems (1995). "CRASH syndrome: clinical spectrum of corpus callosum hypoplasia, retardation, adducted thumbs,

spastic paraparesis and hydrocephalus due to mutations in one single gene, L1." Eur J Hum Genet 3(5): 273-284.

Garaschuk, O., J. Linn, J. Eilers and A. Konnerth (2000). "Large-scale oscillatory calcium waves in the immature cortex." Nat Neurosci 3(5): 452-459.

Garcia, C. A., P. A. McGarry, M. Voirol and C. Duncan (1973). "Neurological involvement in the Smith-Lemli-Opitz syndrome: clinical and neuropathological findings." Dev Med Child Neurol 15(1): 48-55.

Garieri, M., G. Stamoulis, X. Blanc, E. Falconnet, P. Ribaux, C. Borel, F. Santoni and S. E. Antonarakis (2018). "Extensive cellular heterogeneity of X inactivation revealed by single-cell allele-specific expression in human fibroblasts." Proc Natl Acad Sci U S A 115(51): 13015-13020.

Gennarino, V. A., E. E. Palmer, L. M. McDonell, L. Wang, C. J. Adamski, A. Koire, L. See, C. A. Chen, C. P. Schaaf, J. A. Rosenfeld, J. A. Panzer, U. Moog, S. Hao, A. Bye, E. P. Kirk, P. Stankiewicz, A. M. Breman, A. McBride, T. Kandula, H. A. Dubbs, R. Macintosh, M. Cardamone, Y. Zhu, K. Ying, K. R. Dias, M. T. Cho, L. B. Henderson, B. Baskin, P. Morris, J. Tao, M. J. Cowley, M. E. Dinger, T. Roscioli, O. Caluseriu, O. Suchowersky, R. K. Sachdev, O. Lichtarge, J. Tang, K. M. Boycott, J. L. Holder, Jr. and H. Y. Zoghbi (2018). "A Mild PUM1 Mutation Is Associated with Adult-Onset Ataxia, whereas Haploinsufficiency Causes Developmental Delay and Seizures." Cell 172(5): 924-936 e911.

Glass, H. C., G. M. Shaw, C. Ma and E. H. Sherr (2008). "Agenesis of the corpus callosum in California 1983-2003: a population-based study." Am J Med Genet A 146A(19): 2495-2500.

Gleeson, J. G., K. M. Allen, J. W. Fox, E. D. Lamperti, S. Berkovic, I. Scheffer, E. C. Cooper, W. B. Dobyns, S. R. Minnerath, M. E. Ross and C. A. Walsh (1998). "Doublecortin, a brain-specific

gene mutated in human X-linked lissencephaly and double cortex syndrome, encodes a putative signaling protein." Cell 92(1): 63-72.

Gonzalez, G. A., P. Menzel, J. Leonard, W. H. Fischer and M. R. Montminy (1991). "Characterization of motifs which are critical for activity of the cyclic AMP-responsive transcription factor CREB." Mol Cell Biol 11(3): 1306-1312.

Gonzalez, G. A. and M. R. Montminy (1989). "Cyclic AMP stimulates somatostatin gene transcription by phosphorylation of CREB at serine 133." Cell 59(4): 675-680.

Graham, V., J. Khudyakov, P. Ellis and L. Pevny (2003). "SOX2 functions to maintain neural progenitor identity." Neuron 39(5): 749-765.

Grover, V. K., J. G. Valadez, A. B. Bowman and M. K. Cooper (2011). "Lipid modifications of Sonic hedgehog ligand dictate cellular reception and signal response." PLoS One 6(7): e21353.

Hayhurst, M., B. B. Gore, M. Tessier-Lavigne and S. K. McConnell (2008). "Ongoing sonic hedgehog signaling is required for dorsal midline formation in the developing forebrain." Dev Neurobiol 68(1): 83-100.

Hetts, S. W., E. H. Sherr, S. Chao, S. Gobuty and A. J. Barkovich (2006). "Anomalies of the corpus callosum: an MR analysis of the phenotypic spectrum of associated malformations." AJR Am J Roentgenol 187(5): 1343-1348.

Hewitt, W. (1962). "The development of the human corpus callosum." J Anat 96: 355-358.

Hotchkiss, L., S. Donkervoort, M. E. Leach, P. Mohassel, D. X. Bharucha-Goebel, N. Bradley, D. Nguyen, Y. Hu, J. Gurgel-Giannetti and C. G. Bonnemann (2016). "Novel De Novo Mutations in KIF1A as a Cause of Hereditary Spastic Paraplegia With Progressive Central Nervous System Involvement." J Child Neurol 31(9): 1114-1119.

Huffman, K. J., S. Garel and J. L. Rubenstein (2004). "Fgf8 regulates the development of intra-neocortical projections." J Neurosci 24(41): 8917-8923.

Innocenti, G. M. and D. J. Price (2005). "Exuberance in the development of cortical networks." Nat Rev Neurosci 6(12): 955-965.

Iossifov, I., B. J. O'Roak, S. J. Sanders, M. Ronemus, N. Krumm, D. Levy, H. A. Stessman, K. T. Witherspoon, L. Vives, K. E. Patterson, J. D. Smith, B. Paeper, D. A. Nickerson, J. Dea, S. Dong, L. E. Gonzalez, J. D. Mandell, S. M. Mane, M. T. Murtha, C. A. Sullivan, M. F. Walker, Z. Waqar, L. Wei, A. J. Willsey, B. Yamrom, Y. H. Lee, E. Grabowska, E. Dalkic, Z. Wang, S. Marks, P. Andrews, A. Leotta, J. Kendall, I. Hakker, J. Rosenbaum, B. Ma, L. Rodgers

, J. Troge, G. Narzisi, S. Yoon, M. C. Schatz, K. Ye, W. R. McCombie, J. Shendure, E. E. Eichler, M. W. State and M. Wigler (2014). "The contribution of de novo coding mutations to autism spectrum disorder." Nature 515(7526): 216-221.

Jamuar, S. S. and C. A. Walsh (2015). "Genomic variants and variations in malformations of cortical development." Pediatr Clin North Am 62(3): 571-585.

Jiang, L., Z. H. Gu, Z. X. Yan, X. Zhao, Y. Y. Xie, Z. G. Zhang, C. M. Pan, Y. Hu, C. P. Cai, Y. Dong, J. Y. Huang, L. Wang, Y. Shen, G. Meng, J. F. Zhou, J. D. Hu, J. F. Wang, Y. H. Liu, L. H. Yang, F. Zhang, J. M. Wang, Z. Wang, Z. G. Peng, F. Y. Chen, Z. M. Sun, H. Ding, J. M. Shi, J. Hou, J. S. Yan, J. Y. Shi, L. Xu, Y. Li, J. Lu, Z. Zheng, W. Xue, W. L. Zhao, Z. Chen and S. J. Chen (2015). "Exome sequencing identifies somatic mutations of DDX3X in natural killer/T-cell lymphoma." Nat Genet 47(9): 1061-1066.

Jira, P. E., H. R. Waterham, R. J. Wanders, J. A. Smeitink, R. C. Sengers and R. A. Wevers (2003). "Smith-Lemli-Opitz syndrome and the DHCR7 gene." Ann Hum Genet 67(Pt 3): 269-280.

Jones, D. T., N. Jager, M. Kool, T. Zichner, B. Hutter, M. Sultan, Y. J. Cho, T. J. Pugh, V. Hovestadt, A. M. Stutz, T. Rausch, H. J. Warnatz, M. Ryzhova, S. Bender, D. Sturm, S. Pleier, H. Cin, E. Pfaff, L. Sieber, A. Wittmann, M. Remke, H. Witt, S. Hutter, T. Tzaridis, J. Weischenfeldt, B. Raeder, M. Avci, V. Amstislavskiy, M. Zapatka, U. D. Weber, Q. Wang, B. Lasitschka, C. C. Bartholomae, M. Schmidt, C. von Kalle, V. Ast, C. Lawerenz, J. Eils, R. Kabbe, V. Benes, P. van Sluis, J. Koster, R. Volckmann, D. Shih, M. J. Betts, R. B. Russell, S. Coco, G. P. Tonini, U. Schuller, V. Hans, N. Graf, Y. J. Kim, C. Monoranu, W. Roggendorf, A. Unterberg, C. Herold-Mende, T. Milde, A. E. Kulozik, A. von Deimling, O. Witt, E. Maass, J. Rossler, M. Ebinger, M. U. Schuhmann, M. C. Fruhwald, M. Hasselblatt, N. Jabado, S. Rutkowski, A. O. von Bueren, D. Williamson, S. C. Clifford, M. G. McCabe, V. P. Collins, S. Wolf, S. Wiemann, H. Lehrach, B. Brors, W. Scheurlen, J. Felsberg, G. Reifenberger, P. A. Northcott, M. D. Taylor, M. Meyerson, S. L. Pomeroy, M. L. Yaspo, J. O. Korbel, A. Korshunov, R. Eils, S. M. Pfister and P. Lichter (2012). "Dissecting the genomic complexity underlying medulloblastoma." Nature 488(7409): 100-105.

Kanai, Y., N. Dohmae and N. Hirokawa (2004). "Kinesin transports RNA: isolation and characterization of an RNA-transporting granule." Neuron 43(4): 513-525.

Kasahara, J., K. Fukunaga and E. Miyamoto (1999). "Differential effects of a calcineurin inhibitor on glutamate-induced phosphorylation of Ca2+/calmodulin-dependent protein kinases in cultured rat hippocampal neurons." J Biol Chem 274(13): 9061-9067.

Kellaris, G., K. Khan, S. M. Baig, I. C. Tsai, F. M. Zamora, P. Ruggieri, M. R. Natowicz and N. Katsanis (2018). "A hypomorphic inherited pathogenic variant in DDX3X causes male intellectual disability with additional neurodevelopmental and neurodegenerative features." Hum Genomics 12(1): 11.

Kotov, A. A., O. M. Olenkina, M. V. Kibanov and L. V. Olenina (2016). "RNA helicase Belle (DDX3) is essential for male germline stem cell maintenance and division in Drosophila." Biochim Biophys Acta 1863(6 Pt A): 1093-1105.

Kowalczyk, T., A. Pontious, C. Englund, R. A. Daza, F. Bedogni, R. Hodge, A. Attardo, C. Bell, W. B. Huttner and R. F. Hevner (2009). "Intermediate neuronal progenitors (basal progenitors) produce pyramidal-projection neurons for all layers of cerebral cortex." Cereb Cortex 19(10): 2439-2450.

Lai, M. C., Y. H. Lee and W. Y. Tarn (2008). "The DEAD-box RNA helicase DDX3 associates with export messenger ribonucleoproteins as well as tip-associated protein and participates in translational control." Mol Biol Cell 19(9): 3847-3858.

Leone, D. P., W. E. Heavner, E. A. Ferenczi, G. Dobreva, J. R. Huguenard, R. Grosschedl and S. K. McConnell (2015). "Satb2 Regulates the Differentiation of Both Callosal and Subcerebral Projection Neurons in the Developing Cerebral Cortex." Cereb Cortex 25(10): 3406-3419.

Li, Q., P. Zhang, C. Zhang, Y. Wang, R. Wan, Y. Yang, X. Guo, R. Huo, M. Lin, Z. Zhou and J. Sha (2014). "DDX3X regulates cell survival and cell cycle during mouse early embryonic development." J Biomed Res 28(4): 282-291.

Markmiller, S., S. Soltanieh, K. L. Server, R. Mak, W. Jin, M. Y. Fang, E. C. Luo, F. Krach, D. Yang, A. Sen, A. Fulzele, J. M. Wozniak, D. J. Gonzalez, M. W. Kankel, F. B. Gao, E. J. Bennett, E. Lecuyer and G. W. Yeo (2018). "Context-Dependent and Disease-Specific Diversity in Protein Interactions within Stress Granules." Cell 172(3): 590-604 e513.

Markmiller, S., S. Soltanieh, K. L. Server, R. Mak, W. Jin, M. Y. Fang, E. C. Luo, F. Krach, D. Yang, A. Sen, A. Fulzele, J. M. Wozniak, D. J. Gonzalez, M. W. Kankel, F. B. Gao, E. J.

Bennett, E. Lecuyer and G. W. Yeo (2018). "Context-Dependent and Disease-Specific Diversity in Protein Interactions within Stress Granules." Cell 172(3): 590-604 e513.

Mayer, S., J. Chen, D. Velmeshev, A. Mayer, U. C. Eze, A. Bhaduri, C. E. Cunha, D. Jung, A. Arjun, E. Li, B. Alvarado, S. Wang, N. Lovegren, M. L. Gonzales, L. Szpankowski, A. Leyrat, J. A. A. West, G. Panagiotakos, A. Alvarez-Buylla, M. F. Paredes, T. J. Nowakowski, A. A. Pollen and A. R. Kriegstein (2019). "Multimodal Single-Cell Analysis Reveals Physiological Maturation in the Developing Human Neocortex." Neuron 102(1): 143-158 e147.

Mayr, B. and M. Montminy (2001). "Transcriptional regulation by the phosphorylation-dependent factor CREB." Nat Rev Mol Cell Biol 2(8): 599-609.

McCabe, M. J., C. Gaston-Massuet, V. Tziaferi, L. C. Gregory, K. S. Alatzoglou, M. Signore, E. Puelles, D. Gerrelli, I. S. Farooqi, J. Raza, J. Walker, S. I. Kavanaugh, P. S. Tsai, N. Pitteloud, J. P. Martinez-Barbera and M. T. Dattani (2011). "Novel FGF8 mutations associated with recessive holoprosencephaly, craniofacial defects, and hypothalamo-pituitary dysfunction." J Clin Endocrinol Metab 96(10): E1709-1718.

McKhann, G. M., 2nd, H. J. Wenzel, C. A. Robbins, A. A. Sosunov and P. A. Schwartzkroin (2003). "Mouse strain differences in kainic acid sensitivity, seizure behavior, mortality, and hippocampal pathology." Neuroscience 122(2): 551-561.

Moldrich, R. X., I. Gobius, T. Pollak, J. Zhang, T. Ren, L. Brown, S. Mori, C. De Juan Romero, O. Britanova, V. Tarabykin and L. J. Richards (2010). "Molecular regulation of the developing commissural plate." J Comp Neurol 518(18): 3645-3661.

Monies, D., M. Abouelhoda, M. AlSayed, Z. Alhassnan, M. Alotaibi, H. Kayyali, M. Al-Owain, A. Shah, Z. Rahbeeni, M. A. Al-Muhaizea, H. I. Alzaidan, E. Cupler, S. Bohlega, E. Faqeih, M. Faden, B. Alyounes, D. Jaroudi, E. Goljan, H. Elbardisy, A. Akilan, R. Albar, H. Aldhalaan, S.

Gulab, A. Chedrawi, B. K. Al Saud, W. Kurdi, N. Makhseed, T. Alqasim, H. Y. El Khashab, H. Al-Mousa, A. Alhashem, I. Kanaan, T. Algoufi, K. Alsaleem, T. A. Basha, F. Al-Murshedi, S. Khan, A. Al-Kindy, M. Alnemer, S. Al-Hajjar, S. Alyamani, H. Aldhekri, A. Al-Mehaidib, R. Arnaout, O. Dabbagh, M. Shagrani, D. Broering, M. Tulbah, A. Alqassmi, M. Almugbel, M. AlQuaiz, A. Alsaman, K. Al-Thihli, R. A. Sulaiman, W. Al-Dekhail, A. Alsaegh, F. A. Bashiri, A. Qari, S. Alhomadi, H. Alkuraya, M. Alsebayel, M. H. Hamad, L. Szonyi, F. Abaalkhail, S. M. Al-Mayouf, H. Almojalli, K. S. Alqadi, H. Elsiesy, T. M. Shuaib, M. Z. Seidahmed, I. Abosoudah, H. Akleh, A. AlGhonaium, T. M. Alkharfy, F. Al Mutairi, W. Eyaid, A. Alshanbary, F. R. Sheikh, F. I. Alsohaibani, A. Alsonbul, S. Al Tala, S. Balkhy, R. Bassiouni, A. S. Alenizi, M. H. Hussein, S. Hassan, M. Khalil, B. Tabarki, S. Alshahwan, A. Oshi, Y. Sabr, S. Alsaadoun, M. A. Salih, S. Mohamed, H. Sultana, A. Tamim, M. El-Haj, S. Alshahrani, D. K. Bubshait, M. Alfadhel, T. Faquih, M. El-Kalioby, S. Subhani, Z. Shah, N. Moghrabi, B. F. Meyer and F. S. Alkuraya (2017). "The landscape of genetic diseases in Saudi Arabia based on the first 1000 diagnostic panels and exomes." Hum Genet 136(8): 921-939.

Mroch, A. R., M. Laudenschlager and J. D. Flanagan (2012). "Detection of a novel FH whole gene deletion in the propositus leading to subsequent prenatal diagnosis in a sibship with fumarase deficiency." Am J Med Genet A 158A(1): 155-158.

Mummery-Widmer, J. L., M. Yamazaki, T. Stoeger, M. Novatchkova, S. Bhalerao, D. Chen, G. Dietzl, B. J. Dickson and J. A. Knoblich (2009). "Genome-wide analysis of Notch signalling in Drosophila by transgenic RNAi." Nature 458(7241): 987-992.

Nakata, Y., A. J. Barkovich, M. Wahl, Z. Strominger, R. J. Jeremy, M. Wakahiro, P. Mukherjee and E. H. Sherr (2009). "Diffusion abnormalities and reduced volume of the ventral cingulum bundle in agenesis of the corpus callosum: a 3T imaging study." AJNR Am J Neuroradiol 30(6): 1142-1148.

Nedelsky, N. B. and J. P. Taylor (2019). "Bridging biophysics and neurology: aberrant phase transitions in neurodegenerative disease." Nat Rev Neurol 15(5): 272-286.

Niquille, M., S. Garel, F. Mann, J. P. Hornung, B. Otsmane, S. Chevalley, C. Parras, F. Guillemot, P. Gaspar, Y. Yanagawa and C. Lebrand (2009). "Transient neuronal populations are required to guide callosal axons: a role for semaphorin 3C." PLoS Biol 7(10): e1000230.

Noctor, S. C., A. C. Flint, T. A. Weissman, R. S. Dammerman and A. R. Kriegstein (2001). "Neurons derived from radial glial cells establish radial units in neocortex." Nature 409(6821): 714-720.

Noctor, S. C., V. Martinez-Cerdeno, L. Ivic and A. R. Kriegstein (2004). "Cortical neurons arise in symmetric and asymmetric division zones and migrate through specific phases." Nat Neurosci 7(2): 136-144.

O'Driscoll, M. C., G. C. Black, J. Clayton-Smith, E. H. Sherr and W. B. Dobyns (2010). "Identification of genomic loci contributing to agenesis of the corpus callosum." Am J Med Genet A 152A(9): 2145-2159.

Okada, T., Y. Okumura, J. Motoyama and M. Ogawa (2008). "FGF8 signaling patterns the telencephalic midline by regulating putative key factors of midline development." Dev Biol 320(1): 92-101.

Olivetti, P. R., A. Maheshwari and J. L. Noebels (2014). "Neonatal estradiol stimulation prevents epilepsy in Arx model of X-linked infantile spasms syndrome." Sci Transl Med 6(220): 220ra212.

Osbun, N., J. Li, M. C. O'Driscoll, Z. Strominger, M. Wakahiro, E. Rider, P. Bukshpun, E. Boland, C. H. Spurrell, W. Schackwitz, L. A. Pennacchio, W. B. Dobyns, G. C. Black and E. H.

Sherr (2011). "Genetic and functional analyses identify DISC1 as a novel callosal agenesis candidate gene." Am J Med Genet A 155A(8): 1865-1876.

Osbun, N., J. Li, M. C. O'Driscoll, Z. Strominger, M. Wakahiro, E. Rider, P. Bukshpun, E. Boland, C. H. Spurrell, W. Schackwitz, L. A. Pennacchio, W. B. Dobyns, G. C. Black and E. H. Sherr (2011). "Genetic and functional analyses identify DISC1 as a novel callosal agenesis candidate gene." Am J Med Genet A 155A(8): 1865-1876.

Ozes, A. R., K. Feoktistova, B. C. Avanzino, E. P. Baldwin and C. S. Fraser (2014). "Real-time fluorescence assays to monitor duplex unwinding and ATPase activities of helicases." Nat Protoc 9(7): 1645-1661.

Patel, K. P., T. W. O'Brien, S. H. Subramony, J. Shuster and P. W. Stacpoole (2012). "The spectrum of pyruvate dehydrogenase complex deficiency: clinical, biochemical and genetic features in 371 patients." Mol Genet Metab 106(3): 385-394.

Pek, J. W. and T. Kai (2011). "DEAD-box RNA helicase Belle/DDX3 and the RNA interference pathway promote mitotic chromosome segregation." Proc Natl Acad Sci U S A 108(29): 12007-12012.

Phung, B., M. Ciesla, A. Sanna, N. Guzzi, G. Beneventi, P. Cao Thi Ngoc, M. Lauss, R. Cabrita, E. Cordero, A. Bosch, F. Rosengren, J. Hakkinen, K. Griewank, A. Paschen, K. Harbst, H. Olsson, C. Ingvar, A. Carneiro, H. Tsao, D. Schadendorf, K. Pietras, C. Bellodi and G. Jonsson (2019). "The X-Linked DDX3X RNA Helicase Dictates Translation Reprogramming and Metastasis in Melanoma." Cell Rep 27(12): 3573-3586 e3577.

Piper, M., C. Plachez, O. Zalucki, T. Fothergill, G. Goudreau, R. Erzurumlu, C. Gu and L. J. Richards (2009). "Neuropilin 1-Sema signaling regulates crossing of cingulate pioneering axons during development of the corpus callosum." Cereb Cortex 19 Suppl 1: i11-21.

Polioudakis, D., L. de la Torre-Ubieta, J. Langerman, A. G. Elkins, X. Shi, J. L. Stein, C. K. Vuong, S. Nichterwitz, M. Gevorgian, C. K. Opland, D. Lu, W. Connell, E. K. Ruzzo, J. K. Lowe, T. Hadzic, F. I. Hinz, S. Sabri, W. E. Lowry, M. B. Gerstein, K. Plath and D. H. Geschwind (2019). "A Single-Cell Transcriptomic Atlas of Human Neocortical Development during Mid-gestation." Neuron 103(5): 785-801 e788.

Pugh, T. J., S. D. Weeraratne, T. C. Archer, D. A. Pomeranz Krummel, D. Auclair, J. Bochicchio, M. O. Carneiro, S. L. Carter, K. Cibulskis, R. L. Erlich, H. Greulich, M. S. Lawrence, N. J. Lennon, A. McKenna, J. Meldrim, A. H. Ramos, M. G. Ross, C. Russ, E. Shefler, A. Sivachenko, B. Sogoloff, P. Stojanov, P. Tamayo, J. P. Mesirov, V. Amani, N. Teider, S. Sengupta, J. P. Francois, P. A. Northcott, M. D. Taylor, F. Yu, G. R. Crabtree, A. G. Kautzman, S. B. Gabriel, G. Getz, N. Jager, D. T. Jones, P. Lichter, S. M. Pfister, T. M. Roberts, M. Meyerson, S. L. Pomeroy and Y. J. Cho (2012). "Medulloblastoma exome sequencing uncovers subtype-specific somatic mutations." Nature 488(7409): 106-110.

Quintero-Rivera, F., C. D. Robson, R. E. Reiss, D. Levine, C. B. Benson, J. B. Mulliken and V. E. Kimonis (2006). "Intracranial anomalies detected by imaging studies in 30 patients with Apert syndrome." Am J Med Genet A 140(12): 1337-1338.

Racine, R. J. (1972). "Modification of seizure activity by electrical stimulation. II. Motor seizure." Electroencephalogr Clin Neurophysiol 32(3): 281-294.

Rakic, P. and P. I. Yakovlev (1968). "Development of the corpus callosum and cavum septi in man." J Comp Neurol 132(1): 45-72.

Rash, B. G. and L. J. Richards (2001). "A role for cingulate pioneering axons in the development of the corpus callosum." J Comp Neurol 434(2): 147-157.

Redmond, L., A. H. Kashani and A. Ghosh (2002). "Calcium regulation of dendritic growth via CaM kinase IV and CREB-mediated transcription." Neuron 34(6): 999-1010.

Ren, T., A. Anderson, W. B. Shen, H. Huang, C. Plachez, J. Zhang, S. Mori, S. L. Kinsman and L. J. Richards (2006). "Imaging, anatomical, and molecular analysis of callosal formation in the developing human fetal brain." Anat Rec A Discov Mol Cell Evol Biol 288(2): 191-204.

RK, C. Y., D. Merico, M. Bookman, L. H. J, B. Thiruvahindrapuram, R. V. Patel, J. Whitney, N. Deflaux, J. Bingham, Z. Wang, G. Pellecchia, J. A. Buchanan, S. Walker, C. R. Marshall, M. Uddin, M. Zarrei, E. Deneault, L. D'Abate, A. J. Chan, S. Koyanagi, T. Paton, S. L. Pereira, N. Hoang, W. Engchuan, E. J. Higginbotham, K. Ho, S. Lamoureux, W. Li, J. R. MacDonald, T. Nalpathamkalam, W. W. Sung, F. J. Tsoi, J. Wei, L. Xu, A. M. Tasse, E. Kirby, W. Van Etten, S. Twigger, W. Roberts, I. Drmic, S. Jilderda, B. M. Modi, B. Kellam, M. Szego, C. Cytrynbaum, R. Weksberg, L. Zwaigenbaum, M. Woodbury-Smith, J. Brian, L. Senman, A. Iaboni, K. Doyle-Thomas, A. Thompson, C. Chrysler, J. Leef, T. Savion-Lemieux, I. M. Smith, X. Liu, R. Nicolson, V. Seifer, A. Fedele, E. H. Cook, S. Dager, A. Estes, L. Gallagher, B. A. Malow, J. R. Parr, S. J. Spence, J. Vorstman, B. J. Frey, J. T. Robinson, L. J. Strug, B. A. Fernandez, M. Elsabbagh, M. T. Carter, J. Hallmayer, B. M. Knoppers, E. Anagnostou, P. Szatmari, R. H. Ring, D. Glazer, M. T. Pletcher and S. W. Scherer (2017). "Whole genome sequencing resource identifies 18 new candidate genes for autism spectrum disorder." Nat Neurosci 20(4): 602-611.

Robbins, D. J., D. L. Fei and N. A. Riobo (2012). "The Hedgehog signal transduction network." Sci Signal 5(246): re6.

Robinson, G., M. Parker, T. A. Kranenburg, C. Lu, X. Chen, L. Ding, T. N. Phoenix, E. Hedlund, L. Wei, X. Zhu, N. Chalhoub, S. J. Baker, R. Huether, R. Kriwacki, N. Curley, R. Thiruvenkatam, J. Wang, G. Wu, M. Rusch, X. Hong, J. Becksfort, P. Gupta, J. Ma, J. Easton, B. Vadodaria, A. Onar-Thomas, T. Lin, S. Li, S. Pounds, S. Paugh, D. Zhao, D. Kawauchi, M. F. Roussel, D.

Finkelstein, D. W. Ellison, C. C. Lau, E. Bouffet, T. Hassall, S. Gururangan, R. Cohn, R. S. Fulton, L. L. Fulton, D. J. Dooling, K. Ochoa, A. Gajjar, E. R. Mardis, R. K. Wilson, J. R. Downing, J. Zhang and R. J. Gilbertson (2012). "Novel mutations target distinct subgroups of medulloblastoma." Nature 488(7409): 43-48.

Rosenthal, A., M. Jouet and S. Kenwrick (1992). "Aberrant splicing of neural cell adhesion molecule L1 mRNA in a family with X-linked hydrocephalus." Nat Genet 2(2): 107-112.

Sansom, S. N., D. S. Griffiths, A. Faedo, D. J. Kleinjan, Y. Ruan, J. Smith, V. van Heyningen, J. L. Rubenstein and F. J. Livesey (2009). "The level of the transcription factor Pax6 is essential for controlling the balance between neural stem cell self-renewal and neurogenesis." PLoS Genet 5(6): e1000511.

Sato-Maeda, M., H. Tawarayama, M. Obinata, J. Y. Kuwada and W. Shoji (2006). "Sema3a1 guides spinal motor axons in a cell- and stage-specific manner in zebrafish." Development 133(5): 937-947.

Schell-Apacik, C. C., K. Wagner, M. Bihler, B. Ertl-Wagner, U. Heinrich, E. Klopocki, V. M. Kalscheuer, M. Muenke and H. von Voss (2008). "Agenesis and dysgenesis of the corpus callosum: clinical, genetic and neuroimaging findings in a series of 41 patients." Am J Med Genet A 146A(19): 2501-2511.

Schupper, A., O. Konen, A. Halevy, R. Cohen, S. Aharoni and A. Shuper (2017). "Thick Corpus Callosum in Children." J Clin Neurol 13(2): 170-174.

Sharma, D. and E. Jankowsky (2014). "The Ded1/DDX3 subfamily of DEAD-box RNA helicases." Crit Rev Biochem Mol Biol 49(4): 343-360.

Sharma, S., S. Puttachary, A. Thippeswamy, A. G. Kanthasamy and T. Thippeswamy (2018). "Status Epilepticus: Behavioral and Electroencephalography Seizure Correlates in Kainate Experimental Models." Front Neurol 9: 7.

Sherr, E. H. (2003). "The ARX story (epilepsy, mental retardation, autism, and cerebral malformations): one gene leads to many phenotypes." Curr Opin Pediatr 15(6): 567-571.

Shih, J. W., T. Y. Tsai, C. H. Chao and Y. H. Wu Lee (2008). "Candidate tumor suppressor DDX3 RNA helicase specifically represses cap-dependent translation by acting as an eIF4E inhibitory protein." Oncogene 27(5): 700-714.

Shih, J. W., W. T. Wang, T. Y. Tsai, C. Y. Kuo, H. K. Li and Y. H. Wu Lee (2012). "Critical roles of RNA helicase DDX3 and its interactions with eIF4E/PABP1 in stress granule assembly and stress response." Biochem J 441(1): 119-129.

Sholl, D. A. (1953). "Dendritic organization in the neurons of the visual and motor cortices of the cat." J Anat 87(4): 387-406.

Shu, T., K. G. Butz, C. Plachez, R. M. Gronostajski and L. J. Richards (2003). "Abnormal development of forebrain midline glia and commissural projections in Nfia knock-out mice." J Neurosci 23(1): 203-212.

Slaney, S. F., M. Oldridge, J. A. Hurst, G. M. Moriss-Kay, C. M. Hall, M. D. Poole and A. O. Wilkie (1996). "Differential effects of FGFR2 mutations on syndactyly and cleft palate in Apert syndrome." Am J Hum Genet 58(5): 923-932.

Snijders Blok, L., E. Madsen, J. Juusola, C. Gilissen, D. Baralle, M. R. Reijnders, H. Venselaar, C. Helsmoortel, M. T. Cho, A. Hoischen, L. E. Vissers, T. S. Koemans, W. Wissink-Lindhout, E. E. Eichler, C. Romano, H. Van Esch, C. Stumpel, M. Vreeburg, E. Smeets, K. Oberndorff, B. W.

van Bon, M. Shaw, J. Gecz, E. Haan, M. Bienek, C. Jensen, B. L. Loeys, A. Van Dijck, A. M. Innes, H. Racher, S. Vermeer, N. Di Donato, A. Rump, K. Tatton-Brown, M. J. Parker, A. Henderson, S. A. Lynch, A. Fryer, A. Ross, P. Vasudevan, U. Kini, R. Newbury-Ecob, K. Chandler, A. Male, D. D. D. Study, S. Dijkstra, J. Schieving, J. Giltay, K. L. van Gassen, J. Schuurs-Hoeijmakers, P. L. Tan, I. Pediaditakis, S. A. Haas, K. Retterer, P. Reed, K. G. Monaghan, E. Haverfield, M. Natowicz, A. Myers, M. C. Kruer, Q. Stein, K. A. Strauss, K. W. Brigatti, K. Keating, B. K. Burton, K. H. Kim, J. Charrow, J. Norman, A. Foster-Barber, A. D. Kline, A. Kimball, E. Zackai, M. Harr, J. Fox, J. McLaughlin, K. Lindstrom, K. M. Haude, K. van Roozendaal, H. Brunner, W. K. Chung, R. F. Kooy, R. Pfundt, V. Kalscheuer, S. G. Mehta, N. Katsanis and T. Kleefstra (2015). "Mutations in DDX3X Are a Common Cause of Unexplained Intellectual Disability with Gender-Specific Effects on Wnt Signaling." Am J Hum Genet 97(2): 343-352.

Sotiriadis, A. and G. Makrydimas (2012). "Neurodevelopment after prenatal diagnosis of isolated agenesis of the corpus callosum: an integrative review." Am J Obstet Gynecol 206(4): 337 e331-335.

Srivastava, D. P., K. M. Woolfrey, K. A. Jones, C. T. Anderson, K. R. Smith, T. A. Russell, H. Lee, M. V. Yasvoina, D. L. Wokosin, P. H. Ozdinler, G. M. Shepherd and P. Penzes (2012). "An autism-associated variant of Epac2 reveals a role for Ras/Epac2 signaling in controlling basal dendrite maintenance in mice." PLoS Biol 10(6): e1001350.

Tagawa, Y. and T. Hirano (2012). "Activity-dependent callosal axon projections in neonatal mouse cerebral cortex." Neural Plast 2012: 797295.

Taverna, E., M. Gotz and W. B. Huttner (2014). "The cell biology of neurogenesis: toward an understanding of the development and evolution of the neocortex." Annu Rev Cell Dev Biol 30: 465-502.

Tischfield, M. A., H. N. Baris, C. Wu, G. Rudolph, L. Van Maldergem, W. He, W. M. Chan, C. Andrews, J. L. Demer, R. L. Robertson, D. A. Mackey, J. B. Ruddle, T. D. Bird, I. Gottlob, C. Pieh, E. I. Traboulsi, S. L. Pomeroy, D. G. Hunter, J. S. Soul, A. Newlin, L. J. Sabol, E. J. Doherty, C. E. de Uzcategui, N. de Uzcategui, M. L. Collins, E. C. Sener, B. Wabbels, H. Hellebrand, T. Meitinger, T. de Berardinis, A. Magli, C. Schiavi, M. Pastore-Trossello, F. Koc, A. M. Wong, A. V. Levin, M. T. Geraghty, M. Descartes, M. Flaherty, R. V. Jamieson, H. U. Moller, I. Meuthen, D. F. Callen, J. Kerwin, S. Lindsay, A. Meindl, M. L. Gupta, Jr., D. Pellman and E. C. Engle (2010). "Human TUBB3 mutations perturb microtubule dynamics, kinesin interactions, and axon guidance." Cell 140(1): 74-87.

Tokumitsu, H., D. A. Brickey, J. Glod, H. Hidaka, J. Sikela and T. R. Soderling (1994). "Activation mechanisms for Ca2+/calmodulin-dependent protein kinase IV. Identification of a brain CaM-kinase IV kinase." J Biol Chem 269(46): 28640-28647.

Valentin-Vega, Y. A., Y. D. Wang, M. Parker, D. M. Patmore, A. Kanagaraj, J. Moore, M. Rusch, D. Finkelstein, D. W. Ellison, R. J. Gilbertson, J. Zhang, H. J. Kim and J. P. Taylor (2016). "Cancer-associated DDX3X mutations drive stress granule assembly and impair global translation." Sci Rep 6: 25996.

Vos, Y. J., H. E. de Walle, K. K. Bos, J. A. Stegeman, A. M. Ten Berge, M. Bruining, M. C. van Maarle, M. W. Elting, N. S. den Hollander, B. Hamel, A. M. Fortuna, L. E. Sunde, I. Stolte-Dijkstra, C. T. Schrander-Stumpel and R. M. Hofstra (2010). "Genotype-phenotype correlations in L1 syndrome: a guide for genetic counselling and mutation analysis." J Med Genet 47(3): 169-175.

Wang, X., J. E. Posey, J. A. Rosenfeld, C. A. Bacino, F. Scaglia, L. Immken, J. M. Harris, S. E. Hickey, T. M. Mosher, A. Slavotinek, J. Zhang, J. Beuten, M. S. Leduc, W. He, F. Vetrini, M. A. Walkiewicz, W. Bi, R. Xiao, P. Liu, Y. Shao, A. Gezdirici, E. Y. Gulec, Y. Jiang, S. A. Darilek, A.

W. Hansen, M. M. Khayat, D. Pehlivan, J. Piard, D. M. Muzny, N. Hanchard, J. W. Belmont, L. Van Maldergem, R. A. Gibbs, M. K. Eldomery, Z. C. Akdemir, A. M. Adesina, S. Chen, Y. C. Lee, N. Undiagnosed Diseases, B. Lee, J. R. Lupski, C. M. Eng, F. Xia, Y. Yang, B. H. Graham and P. Moretti (2018). "Phenotypic expansion in DDX3X - a common cause of intellectual disability in females." Ann Clin Transl Neurol 5(10): 1277-1285.

Wieland, I., S. Jakubiczka, P. Muschke, M. Cohen, H. Thiele, K. L. Gerlach, R. H. Adams and P. Wieacker (2004). "Mutations of the ephrin-B1 gene cause craniofrontonasal syndrome." Am J Hum Genet 74(6): 1209-1215.

Wieland, I., W. Reardon, S. Jakubiczka, B. Franco, W. Kress, C. Vincent-Delorme, P. Thierry, M. Edwards, R. Konig, C. Rusu, S. Schweiger, E. Thompson, S. Tinschert, F. Stewart and P. Wieacker (2005). "Twenty-six novel EFNB1 mutations in familial and sporadic craniofrontonasal syndrome (CFNS)." Hum Mutat 26(2): 113-118.

Wilkie, A. O., S. F. Slaney, M. Oldridge, M. D. Poole, G. J. Ashworth, A. D. Hockley, R. D. Hayward, D. J. David, L. J. Pulleyn, P. Rutland and *et al*. (1995). "Apert syndrome results from localized mutations of FGFR2 and is allelic with Crouzon syndrome." Nat Genet 9(2): 165-172.

Zahrani, F., M. A. Aldahmesh, M. J. Alshammari, S. A. Al-Hazzaa and F. S. Alkuraya (2013). "Mutations in c12orf57 cause a syndromic form of colobomatous microphthalmia." Am J Hum Genet 92(3): 387-391.

Zahrani, F., M. A. Aldahmesh, M. J. Alshammari, S. A. Al-Hazzaa and F. S. Alkuraya (2013). "Mutations in c12orf57 cause a syndromic form of colobomatous microphthalmia." Am J Hum Genet 92(3): 387-391.

Zech, M., D. D. Lam, S. Weber, R. Berutti, K. Polakova, P. Havrankova, A. Fecikova, T. M. Strom, E. Ruzicka, R. Jech and J. Winkelmann (2018). "A unique de novo gain-of-function

variant in CAMK4 associated with intellectual disability and hyperkinetic movement disorder." Cold Spring Harb Mol Case Stud 4(6).

Zhang, Q., L. Zhang, B. Wang, C. Y. Ou, C. T. Chien and J. Jiang (2006). "A hedgehog-induced BTB protein modulates hedgehog signaling by degrading Ci/Gli transcription factor." Dev Cell 10(6): 719-729.

Zhao, H., T. Maruyama, Y. Hattori, N. Sugo, H. Takamatsu, A. Kumanogoh, R. Shirasaki and N. Yamamoto (2011). "A molecular mechanism that regulates medially oriented axonal growth of upper layer neurons in the developing neocortex." J Comp Neurol 519(5): 834-848.

Zolotushko, J., H. Flusser, B. Markus, I. Shelef, Y. Langer, M. Heverin, I. Bjorkhem, S. Sivan and O. S. Birk (2011). "The desmosterolosis phenotype: spasticity, microcephaly and micrognathia with agenesis of corpus callosum and loss of white matter." Eur J Hum Genet 19(9): 942-946.

Publishing Agreement

It is the policy of the University to encourage the distribution of all theses, dissertations, and manuscripts. Copies of all UCSF theses, dissertations, and manuscripts will be routed to the library via the Graduate Division. The library will make all theses, dissertations, and manuscripts accessible to the public and will preserve these to the best of their abilities, in perpetuity.

Please sign the following statement:

I hereby grant permission to the Graduate Division of the University of California, San Francisco to release copies of my thesis, dissertation, or manuscript to the Campus Library to provide access and preservation, in whole or in part, in perpetuity.

DocuSigned by:
Ruiji Jiang
CB868E09E1B54F7...

Author Signature

11/23/2019

Date